

# Hardware Impairments Aware Transceiver Design for Full-Duplex Amplify-and-Forward MIMO Relaying

Omid Taghizadeh, *Student Member, IEEE*, Ali Cagatay Cirik, *Member, IEEE*, Rudolf Mathar, *Senior Member, IEEE*

**Abstract**—In this work we study the behavior of a full-duplex (FD) and amplify-and-forward (AF) relay with multiple antennas, where hardware impairments of the FD relay transceiver is taken into account. Due to the inter-dependency of the transmit relay power on each antenna and the residual self-interference in an AF-FD relay, we observe a *distortion loop* that degrades the system performance when the relay dynamic range is not high. In this regard, we analyze the relay function in presence of the hardware inaccuracies and an optimization problem is formulated to maximize the signal to distortion-plus-noise ratio (SDNR), under relay and source transmit power constraints. Due to the problem complexity, we propose a gradient-projection-based (GP) algorithm to obtain an optimal solution. Moreover, a non-alternating sub-optimal solution is proposed by assuming a rank-1 relay amplification matrix, and separating the design of the relay process into multiple stages (MuStR1). The proposed MuStR1 method is then enhanced by introducing an alternating update over the optimization variables, denoted as AltMuStR1 algorithm. It is observed that compared to GP, (Alt)MuStR1 algorithms significantly reduce the required computational complexity at the expense of a slight performance degradation. Finally, the proposed methods are evaluated under various system conditions, and compared with the methods available in the current literature. In particular, it is observed that as the hardware impairments increase, or for a system with a high transmit power, the impact of applying a distortion-aware design is significant.

## I. INTRODUCTION

**F**ULL-DUPLEX (FD) operation, as a transceiver's capability to transmit and receive at the same time and frequency, is known with the potential to approach various requirements of future communication systems (5G), e.g., improved spectral efficiency and end-to-end latency [2]. Nevertheless, such systems have been long considered to be practically infeasible due to the inherent self-interference. In theory, since each node is aware of its own transmitted signal, the interference from the loopback path can be estimated and suppressed. However, in practice this procedure is challenging due to the high strength of the self-interference channel compared to the desired communication path, up to 100 dB [3]. Recently, specialized self-interference cancellation (SIC) techniques [4]–[7] have provided an adequate level of isolation between transmit (Tx) and receive (Rx) directions to facilitate an FD communication

and motivated a wide range of related applications, see, e.g., [2], [8]. A common idea of the such SIC techniques is to attenuate the main interference paths in RF domain, i.e., prior to down-conversion, so that the remaining self-interference can be processed in the effective dynamic range of the analog-to-digital converter (ADC) and further attenuated in the baseband, i.e., digital domain. While the aforementioned SIC techniques have provided successful demonstrations for specific scenarios, e.g., [6], it is easy to observe that the obtained cancellation level may vary for different realistic conditions. This mainly includes *i*) aging and inaccuracy of the hardware components, e.g., ADC and digital-to-analog-converter (DAC) noise, power amplifier and oscillator phase noise in analog domain, as well as *ii*) inaccurate estimation of the remaining interference paths due to the limited channel coherence time. As a result, it is essential to take into account the aforementioned inaccuracies to obtain a design which remains efficient under realistic situations.

In this work we are focusing on the application of FD capability on a classic relaying system, where the relay node has multiple antennas and suffers from the effects of hardware inaccuracy. An FD relay is capable of receiving the signal from the source, while simultaneously communicating to the destination. This capability, not only reduces the required time slots in order to accomplish an end to end communication, but also reduces the end to end latency compared to the known Time Division Duplex (TDD)-based half-duplex (HD) relays. In the early work by Riihonen. et. al. [9] the relay operation with a generic processing protocol is modeled, and many insights have been provided regarding the multiple-antenna strategies for reducing the self-interference power. The design methodologies and performance evaluation for FD relays with decode-and-forward (DF) operation have been then studied, see e.g., [10]–[14], taking into account the effects of the hardware impairments, as well as channel estimation errors in digital domain. For the FD relaying systems with amplify-and-forward (AF) operation, single antenna relaying scenarios are studied in [15]–[20]. In the aforementioned works the effect of the linear inaccuracies in digital domain have been incorporated in [17], where the hardware imperfections from analog domain components have been addressed in [15], [16], following the model in [3], [10], and in [18] following the proposed model in [21]. The work in [18] is then extended by [19] to enhance the physical layer security in the presence of an Eavesdropper.

While the aforementioned literature introduces the importance of an accurate transceiver modeling with respect to the effects of hardware impairments for an AF-FD relay, such works are not yet extended for the relays with multiple anten-

O. Taghizadeh and R. Mathar are with the Institute for Theoretical Information Technology, RWTH Aachen University, Aachen, 52074, Germany (email: {taghizadeh, mathar}@ti.rwth-aachen.de).

A. C. Cirik is with the Department of Electrical and Computer Engineering, University of British Columbia, Vancouver, BC V6T 1Z4, Canada (email: cirik@ece.ubc.ca).

Part of this work has been presented in ISWCS'16, the 2016 International Symposium on Wireless Communication Systems [1].

nas. This stems from the fact that in an AF-FD relay, the interdependent behavior of the transmit power from the relay and the residual self-interference intensity results in a distortion-loop effect, see Subsection II-C. The aforementioned effect results in a rather complicated mathematical description when relay is equipped with multiple antennas. As a result, related studies resort to simplified models to reduce the consequent design complexity. In [22]–[34] a multiple-antenna AF-FD relay system is studied, where the impact of the residual self-interference is modeled as a known and purely linear system. As a result it is assumed that the self-interference signal can be canceled via estimating and subtracting the interference term in the receiver [22]–[24], or can be reduced via optimized transmit/receive linear strategies, e.g., spatial zero-forcing of the self-interference signal where the number of transmit antennas exceeds the number of receive antennas at the relay [25]–[30]. For the scenarios where the number of transmit antennas is not higher than the receive antennas, a general framework is proposed in [31], [32], where a perfect SIC is assumed via a combined analog/digital SIC scheme on the condition that the self-interference power does not exceed a certain threshold. In [33], [34] the impact of residual self-interference is considered in the design of the relay amplification strategy, however, following a perfect hardware assumption where the residual self-interference signal is related to the transmitted signal via a known linear function. To the best of the authors knowledge, the impact of the hardware distortions, as such extensively studied for FD-DF relaying systems [10]–[14], is not yet addressed for FD-AF relays in the available literature.

### A. Contribution

In this work we study a multiple-input-multiple-output (MIMO) AF-FD relay, where the distortions resulting from hardware inaccuracies in the receiver and transmit chains are jointly taken into account. Our goal is to improve the end-to-end performance, in terms of signal-to-distortion-plus-noise ratio (SDNR), via optimized linear transmit/receive strategies. The main contributions of this paper are as follows:

- In Section II and Section III the relay operation is analyzed by taking into account the effects of transmit and receiver chain distortions, and the resulting distortion loop effect is elaborated. Furthermore, an SDNR maximization problem is formulated.
- In order to tackle the intractable nature of the formulated problem, a gradient-projection (GP) based solution is proposed in Section IV to act as a benchmark for the achievable performance.
- In order to reduce the computational complexity, as required by the proposed GP method, a sub-optimal Multi-Stage Rank-1 (MuStR1) solution is provided in Section V, by assuming a rank-1 relay amplification matrix and separating the design of the relay process into multiple stages. In this regard, a non-alternating algorithm is proposed by locally maximizing the resulting SDNR for each stage. Moreover, the performance of MuStR1 is improved by introducing an alternating

update (AltMuStR1), at the cost of a slightly higher computational complexity.

- Finally, the behavior of the aforementioned strategies are evaluated for various system parameters via numerical simulations and the main conclusions are summarized, respectively in Section VIII and Section IX.

### B. Mathematical Notation:

Throughout this paper, column vectors and matrices are denoted as lower-case and upper-case bold letters, respectively. The rank of a matrix, expectation, trace, transpose, conjugate, Hermitian transpose, determinant and Euclidean norm are denoted by  $\text{rank}(\cdot)$ ,  $\mathbb{E}(\cdot)$ ,  $\text{tr}(\cdot)$ ,  $(\cdot)^T$ ,  $(\cdot)^*$ ,  $(\cdot)^H$ ,  $|\cdot|$ ,  $\|\cdot\|_2$ , respectively. The Kronecker product is denoted by  $\otimes$ . The identity matrix with dimension  $K$  is denoted as  $\mathbf{I}_K$  and  $\text{vec}(\cdot)$  operator stacks the elements of a matrix into a vector, and  $(\cdot)^{-1}$  represents the inverse of a matrix. The sets of real, real and positive, complex, natural, and the set  $\{1 \dots K\}$  are respectively denoted by  $\mathbb{R}$ ,  $\mathbb{R}^+$ ,  $\mathbb{C}$ ,  $\mathbb{N}$  and  $\mathbb{F}_K$ .  $[\mathbf{A}_i]_{i \in \mathbb{F}_K}$  denotes a tall matrix, obtained by stacking the matrices  $\mathbf{A}_i$ ,  $i \in \mathbb{F}_K$ . The set of all positive semi-definite matrices is denoted by  $\mathcal{H}$ .  $\perp$  represents statistical independence.  $\lambda_{\max}(\mathbf{A})$  calculates the dominant eigenvector of  $\mathbf{A}$ .  $x^*$  is the value of the variable  $x$  at optimality.

## II. SYSTEM MODEL

We investigate a system where a single-antenna HD source communicates with an HD destination node equipped with  $M_d$  antennas, with a help of an FD relay. The relay is assumed to have  $M_t$  ( $M_r$ ) transmit (receive) antennas, and operates in AF mode. The channels between the source and the relay, between the relay and the destination, and between the source and the destination are denoted as  $\mathbf{h}_{sr} \in \mathbb{C}^{M_t}$ ,  $\mathbf{H}_{rd} \in \mathbb{C}^{M_d \times M_t}$ , and  $\mathbf{h}_{sd} \in \mathbb{C}^{M_d}$ , respectively. The self-interference channel, which is the channel between the relay's transmit and receive ends is denoted as  $\mathbf{H}_{rr} \in \mathbb{C}^{M_r \times M_t}$ . All channels are following the flat-fading model.

### A. Source-to-Relay Communication

The relay continuously receives and amplifies the received signal from the source, while estimating and subtracting the loopback self-interference signal from its own transmitter, see Fig. 1. The received signal at the relay is expressed as

$$\mathbf{r}_{in} = \underbrace{\mathbf{h}_{sr} \sqrt{P_s} s + \mathbf{H}_{rr} \mathbf{r}_{out}}_{=\mathbf{u}_{in}} + \mathbf{e}_{in}, \quad (1)$$

where  $\mathbf{r}_{in} \in \mathbb{C}^{M_r}$  and  $\mathbf{r}_{out} \in \mathbb{C}^{M_t}$  respectively represent the received and transmitted signal from the relay and  $\mathbf{n}_r \sim \mathcal{CN}(\mathbf{0}, \sigma_{nr}^2 \mathbf{I}_{M_r})$  represents the zero-mean additive white complex Gaussian (ZMAWCG) noise at the relay. The transmitted data symbol from the source is denoted as  $s \in \mathbb{C}$ ,  $\mathbb{E}\{|s|^2\} = 1$ .  $P_s \in \mathbb{R}^+$  is the source transmit power and  $\mathbf{u}_{in} \in \mathbb{C}^{M_r}$  represents the *undistorted* received signal at the relay.

The receiver distortion, denoted as  $\mathbf{e}_{in} \in \mathbb{C}^{M_r}$ , represents the combined effects of receiver chain impairments, e.g., limited ADC accuracy, oscillator phase noise, low-noise-amplifier

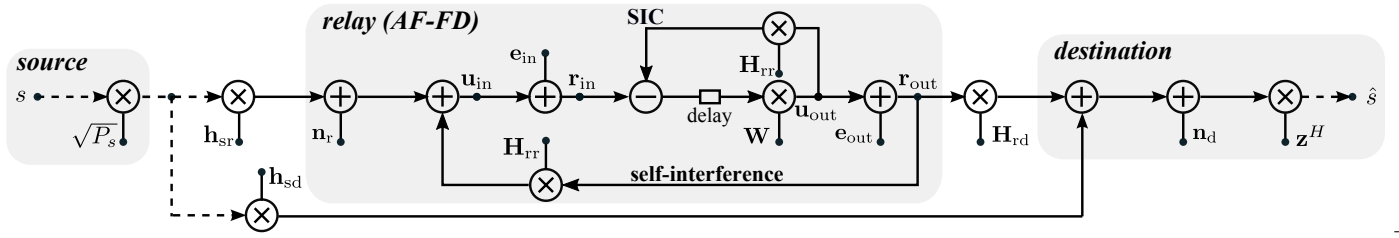


Figure 1. The signal model in an amplify-and-forward FD MIMO relay. The impact of hardware inaccuracies from the transmitter ( $\mathbf{e}_{\text{out}}$ ) and receiver ( $\mathbf{e}_{\text{in}}$ ) chains is observable on the relay process. The bold arrows represent the vector signals while the dashed arrows represent the scalars. See Section II for a detailed description.

(LNA) distortion [10]. Please note that while the aforementioned impairments are usually assumed to be ignorable for an HD transceiver, they play an important role in our system due to high strength of the self-interference path. The known, i.e., distortion-free, part of the self-interference signal is then suppressed in the receiver by utilizing the recently developed SIC techniques in analog and digital domains, e.g., [4], [6]. The remaining signal is then amplified to constitute the relay's output:

$$\mathbf{r}_{\text{out}} = \mathbf{u}_{\text{out}} + \mathbf{e}_{\text{out}}, \quad \mathbf{u}_{\text{out}}(t) = \mathbf{W}\mathbf{r}_{\text{supp}}(t - \tau), \quad (2)$$

$$\mathbf{r}_{\text{supp}} = \mathbf{r}_{\text{in}} - \mathbf{H}_{\text{rr}}\mathbf{u}_{\text{out}}, \quad (3)$$

where  $\mathbf{r}_{\text{supp}} \in \mathbb{C}^{M_r}$  and  $\mathbf{W} \in \mathbb{C}^{M_t \times M_r}$  respectively represent the interference-suppressed version of the received signal and the relay amplification matrix,  $t \in \mathbb{R}^+$  represents the time instance<sup>1</sup>, and  $\tau \in \mathbb{R}^+$  is the relay processing delay, see Subsection II-E3. The *intended* transmit signal is denoted as  $\mathbf{u}_{\text{out}} \in \mathbb{C}^{M_t}$ . Similar to the defined additive distortion in the receiver chains, the combined effects of the transmit chain impairments, e.g., limited DAC accuracy, oscillator phase noise, power amplifier noise, is denoted by  $\mathbf{e}_{\text{out}} \in \mathbb{C}^{M_t}$ . Furthermore, in order to take into account the transmit power limitations we impose

$$\mathbb{E}\{\|\mathbf{r}_{\text{out}}\|_2^2\} \leq P_{r,\text{max}}, \quad P_s \leq P_{s,\text{max}}, \quad (4)$$

where  $P_{r,\text{max}}$  and  $P_{s,\text{max}}$  respectively represents the maximum transmit power from the relay and from the source.

### B. Distortion signal statistics

The impact of hardware elements inaccuracy in each antenna can be closely modeled as an additive distortion signal with a zero-mean complex Gaussian and spatially uncorrelated statistics. This is elaborated in [3, Subsections C], [35], [36] regarding the modeling and characterization of hardware impairments in transmit chains, and in [3, Subsections D], [37] for the receiver chains. This is expressed in the defined relaying system as

$$\mathbf{e}_{\text{in}} \sim \mathcal{CN}(\mathbf{0}, \beta \text{diag}(\mathbb{E}\{\mathbf{u}_{\text{in}}\mathbf{u}_{\text{in}}^H\})), \quad (5)$$

$$\mathbf{e}_{\text{in}}(t) \perp \mathbf{e}_{\text{in}}(t'), \quad \mathbf{e}_{\text{in}}(t) \perp \mathbf{u}_{\text{in}}(t),$$

<sup>1</sup>The argument indicating time instance, i.e.,  $t$ , is dropped for simplicity for signals with a same time reference.

and

$$\mathbf{e}_{\text{out}} \sim \mathcal{CN}(\mathbf{0}, \beta \text{diag}(\mathbb{E}\{\mathbf{u}_{\text{out}}\mathbf{u}_{\text{out}}^H\})), \quad (6)$$

$$\mathbf{e}_{\text{out}}(t) \perp \mathbf{e}_{\text{out}}(t'), \quad \mathbf{e}_{\text{out}}(t) \perp \mathbf{u}_{\text{out}}(t),$$

where  $t \neq t'$  and  $\beta, \kappa \in \mathbb{R}^+$  are the receive and transmit distortion coefficients which respectively relate the *undistorted* receive and transmit signal covariance to the covariance of the corresponding distortion. Note that the defined statistics in (5), (6) indicate that unlike the traditional additive white noise model, a higher transmit (receive) signal power results in a higher transmit (receive) distortion intensity in the corresponding chain. As we will further elaborate, this effect plays an important role in the performance of an AF-FD relay. For more discussions on the used distortion model please see [3], [10]–[12], and the references therein.

### C. Relay-to-destination communication

The transmitted signal from the relay node passes through the relay to destination channel and constitutes the received signal at the destination:

$$\mathbf{y} = \mathbf{H}_{\text{rd}}\mathbf{r}_{\text{out}} + \mathbf{h}_{\text{sd}}\sqrt{P_s}s + \mathbf{n}_d, \quad \hat{s}(t - \tau) = \mathbf{z}^H\mathbf{y}(t), \quad (7)$$

where  $\mathbf{y} \in \mathbb{C}^{M_d}$  is the received signal at the destination, and  $\mathbf{n}_d \sim \mathcal{CN}(\mathbf{0}, \sigma_{\text{nd}}^2 \mathbf{I}_{M_d})$  is the ZMAWCG noise. The linear receiver filter and the estimated received symbol is denoted as  $\mathbf{z} \in \mathbb{C}^{M_d}$  and  $\hat{s}$ , respectively.

### D. Distortion loop

As the transmit power from the relay increases, the power of the error components increase in all receiver chains, see (1) in connection to (5)–(6). On the other hand, these errors are amplified in the relay process and further increase the relay transmit power, see (1) in connection to (3) and (2). The aforementioned effect causes a loop which signifies the problem of residual self-interference for the relays with AF process. In the following section, this impact is analytically studied and an optimization strategy is proposed in order to alleviate this effect.

### E. Remarks

1) *CSI estimation*: In this work we assume that the channel state information (CSI), representing linear signal dependencies in the system, are known by dedicating an adequately long training sequence at the relay, see [10, Subsection III.A]. Therefore, the studied framework serves best for the scenarios with a stationary channel where long training sequences can be utilized, e.g., relay channel in a backhaul directive link with a line-of-sight (LOS) connection [38]. For the scenarios where the CSI can not be accurately obtained, the results of this paper can be treated as theoretical guidelines on the effects of hardware impairments, if CSI were accurately known.

2) *Direct link*: In this work, we assume that the direct link is weak and consider the source-destination path as a source of interference, similar to [10], [17]. For the scenarios where the direct link is strong, it is shown in [39] that the receiver strategy can be gainfully updated as a RAKE receiver [40] to temporally align the desired signal in the direct and relay links. This can be considered as a future extension of the current work.

3) *Processing delay*: The relay output signals, i.e.,  $\mathbf{u}_{\text{out}}$  and  $\mathbf{r}_{\text{out}}$ , are generated from the received signals with a relay processing delay  $\tau$ , see (2). This delay is assumed to be long enough, e.g., more than a symbol duration, such that the source signal is decorrelated, i.e.,  $s(t) \perp s(t-\tau)$  [39], [41]. The zero-mean and independent statistics of the samples from data signal, i.e.,  $s(t)$  and  $s(t-\tau)$ , as well as the noise and distortion signals, are basis for the analysis in the following section.

### III. PERFORMANCE ANALYSIS FOR MIMO AF RELAYING WITH HARDWARE IMPAIRMENTS

In this part, we analyze the end-to-end performance as a function of the relay amplification matrix, i.e.,  $\mathbf{W}$ , receive linear filter at the destination, i.e.,  $\mathbf{z}$ , as well as the transmit power from the source,  $P_s$ . By incorporating (1) and (5)-(6) into (2) and (3) we have

$$\begin{aligned} \mathbf{Q} &= \mathbf{W} \left( P_s \mathbf{h}_{\text{sr}} \mathbf{h}_{\text{sr}}^H + \sigma_{\text{nr}}^2 \mathbf{I}_{M_r} + \mathbb{E} \{ \mathbf{e}_{\text{in}} \mathbf{e}_{\text{in}}^H \} \right. \\ &\quad \left. + \mathbf{H}_{\text{rr}} \mathbb{E} \{ \mathbf{e}_{\text{out}} \mathbf{e}_{\text{out}}^H \} \mathbf{H}_{\text{rr}}^H \right) \mathbf{W}^H \\ &= \mathbf{W} \left( P_s \mathbf{h}_{\text{sr}} \mathbf{h}_{\text{sr}}^H + \sigma_{\text{nr}}^2 \mathbf{I}_{M_r} + \beta \text{diag} \left( \mathbb{E} \{ \mathbf{u}_{\text{in}} \mathbf{u}_{\text{in}}^H \} \right) \right. \\ &\quad \left. + \kappa \mathbf{H}_{\text{rr}} \text{diag}(\mathbf{Q}) \mathbf{H}_{\text{rr}}^H \right) \mathbf{W}^H, \end{aligned} \quad (8)$$

where  $\mathbf{Q} \in \mathcal{H}$  is the covariance matrix of the undistorted transmit signal from the relay, i.e.,  $\mathbf{Q} := \mathbb{E} \{ \mathbf{u}_{\text{out}} \mathbf{u}_{\text{out}}^H \}$ . Furthermore, the undistorted receive covariance matrix can be formulated from (1)-(3) as

$$\mathbb{E} \{ \mathbf{u}_{\text{in}} \mathbf{u}_{\text{in}}^H \} = P_s \mathbf{h}_{\text{sr}} \mathbf{h}_{\text{sr}}^H + \sigma_{\text{nr}}^2 \mathbf{I}_{M_r} + \mathbf{H}_{\text{rr}} \mathbb{E} \{ \mathbf{r}_{\text{out}} \mathbf{r}_{\text{out}}^H \} \mathbf{H}_{\text{rr}}^H. \quad (9)$$

It is worth mentioning that due to the proximity of the Rx and Tx antennas on the FD device, the loopback self-interference signal is much stronger than the desired signal which is coming from a distant location, and hence constitutes the principle part in (9). By recalling (2) and (6) the relay transmit covariance matrix can be formulated as

$$\mathbb{E} \{ \mathbf{r}_{\text{out}} \mathbf{r}_{\text{out}}^H \} = \mathbf{Q} + \kappa \text{diag}(\mathbf{Q}), \quad (10)$$

and consequently from (8) and (9) it follows

$$\mathbf{Q} = \mathbf{W} \mathcal{R}(\mathbf{Q}) \mathbf{W}^H, \quad (11)$$

where

$$\begin{aligned} \mathcal{R}(\mathbf{Q}) &:= P_s \mathbf{h}_{\text{sr}} \mathbf{h}_{\text{sr}}^H + \sigma_{\text{nr}}^2 \mathbf{I}_{M_r} + \beta \text{diag} \left( P_s \mathbf{h}_{\text{sr}} \mathbf{h}_{\text{sr}}^H + \sigma_{\text{nr}}^2 \mathbf{I}_{M_r} \right) \\ &\quad + \beta \text{diag} \left( \mathbf{H}_{\text{rr}} \left( \mathbf{Q} + \kappa \text{diag}(\mathbf{Q}) \right) \mathbf{H}_{\text{rr}}^H \right) \\ &\quad + \kappa \mathbf{H}_{\text{rr}} \text{diag}(\mathbf{Q}) \mathbf{H}_{\text{rr}}^H. \end{aligned} \quad (12)$$

Note that the above derivations (8)-(11) hold as the noise, the desired signal at subsequent symbol durations, and the distortion components are zero-mean and mutually independent. Unfortunately, a direct expression of  $\mathbf{Q}$  in terms of  $\mathbf{W}$  can not be achieved from (11), (12) in the current form. In order to facilitate further analysis we resort to the vectorized presentation of  $\mathbf{Q}$ . By applying the famous matrix equality  $\text{vec}(\mathbf{A}_1 \mathbf{A}_2 \mathbf{A}_3) = (\mathbf{A}_3^T \otimes \mathbf{A}_1) \text{vec}(\mathbf{A}_2)$ , we can write (10) as

$$\text{vec} \left( \mathbb{E} \{ \mathbf{r}_{\text{out}} \mathbf{r}_{\text{out}}^H \} \right) = \left( \mathbf{I}_{M_r^2} + \kappa \mathbf{S}_D^{M_r} \right) \text{vec}(\mathbf{Q}), \quad (13)$$

where  $\mathbf{S}_D^{M_r} \in \{0, 1\}^{M_r^2 \times M_r^2}$  is a selection matrix with one or zero elements such that  $\mathbf{S}_D^{M_r} \text{vec}(\mathbf{Q}) = \text{vec}(\text{diag}(\mathbf{Q}))$ . Similarly from (11) we obtain

$$\text{vec}(\mathbf{Q}) = \left( \mathbf{I}_{M_r^2} - (\mathbf{W}^* \otimes \mathbf{W}) \mathbf{C} \right)^{-1} (\mathbf{W}^* \otimes \mathbf{W}) \mathbf{c}, \quad (14)$$

where

$$\mathbf{C} := \beta \mathbf{S}_D^{M_r} (\mathbf{H}_{\text{rr}}^* \otimes \mathbf{H}_{\text{rr}}) \left( \mathbf{I}_{M_r^2} + \kappa \mathbf{S}_D^{M_r} \right) + \kappa (\mathbf{H}_{\text{rr}}^* \otimes \mathbf{H}_{\text{rr}}) \mathbf{S}_D^{M_r}, \quad (15)$$

$$\mathbf{c} := \left( \mathbf{I}_{M_r^2} + \beta \mathbf{S}_D^{M_r} \right) \text{vec} \left( P_s \mathbf{h}_{\text{sr}} \mathbf{h}_{\text{sr}}^H + \sigma_{\text{nr}}^2 \mathbf{I}_{M_r} \right). \quad (16)$$

The direct dependence of the relay transmit covariance matrix and  $\mathbf{W}$  can be consequently obtained from (14) and (13) as

$$\begin{aligned} \text{vec} \left( \mathbb{E} \{ \mathbf{r}_{\text{out}} \mathbf{r}_{\text{out}}^H \} \right) &= \\ & \left( \mathbf{I}_{M_r^2} + \kappa \mathbf{S}_D^{M_r} \right) \left( \mathbf{I}_{M_r^2} - (\mathbf{W}^* \otimes \mathbf{W}) \mathbf{C} \right)^{-1} (\mathbf{W}^* \otimes \mathbf{W}) \mathbf{c}. \end{aligned} \quad (17)$$

#### A. Optimization problem

In order to formulate the end-to-end link quality, we recall that the noise, the desired signal and the residual interference signals are zero-mean and mutually independent. Hence, the received signal power at the destination, after application of  $\mathbf{z}$ , can be separated as

$$\begin{aligned} P_{\text{des}} &= \mathbb{E} \left\{ \left| \mathbf{z}^H \mathbf{H}_{\text{rd}} \mathbf{W} \mathbf{h}_{\text{sr}} \sqrt{P_s} s \right|^2 \right\} \\ &= P_s \mathbf{z}^H \mathbf{H}_{\text{rd}} \mathbf{W} \mathbf{h}_{\text{sr}} \mathbf{h}_{\text{sr}}^H \mathbf{W}^H \mathbf{H}_{\text{rd}}^H \mathbf{z}, \end{aligned} \quad (18)$$

$$\begin{aligned} P_{\text{tot}} &= \mathbb{E} \left\{ \left| \mathbf{z}^H \left( \mathbf{H}_{\text{rd}} \mathbf{r}_{\text{out}} + \mathbf{h}_{\text{sd}} \sqrt{P_s} s + \mathbf{n}_d \right) \right|^2 \right\} \\ &= \mathbf{z}^H \left( \mathbf{H}_{\text{rd}} \left( \mathbf{Q} + \kappa \text{diag}(\mathbf{Q}) \right) \mathbf{H}_{\text{rd}}^H + \sigma_{\text{nd}}^2 \mathbf{I}_{M_d} + P_s \mathbf{h}_{\text{sd}} \mathbf{h}_{\text{sd}}^H \right) \mathbf{z}, \end{aligned} \quad (19)$$

$$P_{\text{err}} = P_{\text{tot}} - P_{\text{des}}, \quad (20)$$

where  $P_{\text{des}}$  and  $P_{\text{err}}$  respectively represent the power of the desired, and distortion-plus-noise parts of the estimated signal  $\hat{s}$ , and  $P_{\text{tot}} := \mathbb{E}\{|\hat{s}|^2\}$ . The corresponding optimization problem for maximizing the resulting SDNR is written as<sup>2</sup>

$$\begin{aligned} \max_{P_s, \mathbf{z}, \mathbf{W}} \quad & \frac{P_{\text{des}}}{P_{\text{err}}} \quad (21a) \\ \text{s.t.} \quad & (14), \quad \mathbf{Q} \in \mathcal{H}, \quad \text{tr}(\mathbf{Q}) \leq \tilde{P}_{r,\max}, \quad 0 \leq P_s \leq P_{s,\max}, \quad (21b) \end{aligned}$$

where (21b) limits the feasible set of  $\mathbf{W}$  to those resulting in a feasible  $\mathbf{Q}$ . Note that  $\tilde{P}_{r,\max} := \frac{P_{r,\max}}{1+\kappa}$ , and the power constraint in (21b) follows as  $\text{tr}(\mathbf{Q} + \kappa \text{diag}(\mathbf{Q})) = (1 + \kappa)\text{tr}(\mathbf{Q})$ .

As it can be observed, the optimization problem (21a)-(21b) is a non-convex optimization problem and cannot be solved analytically, due to the structure imposed by (14). In order to approach the solution, we propose a GP-based optimization method in the following section.

#### IV. GRADIENT PROJECTION (GP) FOR SDNR MAXIMIZATION

In this part we propose an iterative solution to (21a)-(21b) based on the gradient projection method [3], [42]. In this regard, the optimization variables are updated in the increasing direction of the objective function (21a). When a variable update violates any of the problem constraints, it will be projected into the feasible solution set.

##### A. Iterative update for $\mathbf{W}$

The update rule for  $\mathbf{W}$  is formulated as

$$\mathbf{W}^{(\ell+1)} = \mathcal{P} \left( \mathbf{W}^{(\ell)} + \delta^{(\ell)} \nabla \left( \frac{P_{\text{des}}}{P_{\text{err}}} \right) \right), \quad (22)$$

where  $\mathcal{P}(\cdot)$  represents the projection to the feasible solution space,  $\ell$  represent the iteration index and  $\nabla(\cdot)$  represents the gradient with respect to  $\mathbf{W}^*$ , at the point  $\mathbf{W} = \mathbf{W}^{(\ell)}$ . The step size, representing the size of the variable update is denoted as  $\delta \in \mathbb{R}^+$ .

1) *Update direction for  $\mathbf{W}$* : The update direction in each step is determined following the steepest descent rules [42]. This is done by following the calculated conjugate gradients in (29)-(30), and the fact that

$$\nabla \left( \frac{P_{\text{des}}}{P_{\text{err}}} \right) = \frac{1}{P_{\text{err}}^2} \left( \nabla(P_{\text{des}}) P_{\text{err}} - \nabla(P_{\text{err}}) P_{\text{des}} \right). \quad (23)$$

The value of  $\delta$  is chosen according to the Armijo's step size rule [43], which provides a trade-off between validity of the calculated slope and objective improvement in each step, and ensures convergence to a stationary point.

<sup>2</sup>It is worth mentioning that due to the single stream communication setup, the defined SDNR maximization also results in the maximization of the mutual information between  $s$  and  $\hat{s}$ , assuming a source with Gaussian codewords.

2) *Projection rule*: It is apparent that a variable update may result in a  $\mathbf{W}$  that violates the problem constraints in (21b). More specifically, an updated  $\mathbf{W}$  from (22) may result in a  $\mathbf{Q}$ , calculated from (14), which contains a negative eigenvalue or violates the defined power constraint, see (21b). In order to define the projection rule, let  $\mathbf{W}_{\text{old}}$  and  $\mathbf{Q}_{\text{old}}$  be the updated relay amplification matrix from (22) and the corresponding undistorted transmit covariance, calculated from (14). Moreover, let  $\mathbf{U}_{\text{old}} \mathbf{\Lambda}_{\text{old}} \mathbf{U}_{\text{old}}^H$  be an eigenvalue decomposition of the matrix  $\mathbf{Q}_{\text{old}}$ , such that  $\mathbf{U}_{\text{old}}$  is a unitary matrix, and  $\mathbf{\Lambda}_{\text{old}}$  is a diagonal matrix containing the eigen values. In order to obtain a feasible relay undistorted transmit covariance matrix, i.e.,  $\mathbf{Q}_{\text{new}}$ , we define the following update

$$\mathbf{Q}_{\text{new}} \leftarrow \mathbf{U}_{\text{old}} \underbrace{(\mathbf{\Lambda}_{\text{old}} - \nu \mathbf{I}_{M_t})^+}_{=: \mathbf{\Lambda}_{\text{new}}} \mathbf{U}_{\text{old}}^H, \quad \nu \in \mathbb{R}, \quad (24)$$

where  $(\cdot)^+$  substitutes the negative elements by zero, and  $\nu \in \mathbb{R}$  is the minimum non-negative value that satisfies  $\text{tr}(\mathbf{\Lambda}_{\text{new}}) \leq \tilde{P}_{r,\max}$ , see [3, Subsection III.D] for a similar procedure. The projected version of  $\mathbf{W}_{\text{old}}$ , i.e.,  $\mathbf{W}_{\text{new}}$  is calculated as

$$\mathbf{W}_{\text{new}} \leftarrow \mathbf{Q}_{\text{new}}^{\frac{1}{2}} \mathbf{V} \mathbf{U}_{r,\text{new}} (\mathbf{\Sigma}_{r,\text{new}})^{-\frac{1}{2}} \mathbf{U}_{r,\text{new}}^H, \quad (25)$$

where  $\mathbf{Q}_{\text{new}}^{\frac{1}{2}} = \mathbf{U}_{\text{old}} \mathbf{\Lambda}_{\text{new}}^{\frac{1}{2}} \mathbf{U}_{\text{old}}^H$ ,  $\mathbf{V}$  is an arbitrary unitary matrix such that  $\mathbf{V} \mathbf{V}^H = \mathbf{I}_{M_t}$ , and  $\mathbf{U}_{r,\text{new}} \mathbf{\Sigma}_{r,\text{new}} \mathbf{U}_{r,\text{new}}^H$  is the eigenvalue decomposition of  $\mathcal{R}(\mathbf{Q}_{\text{new}})$ , see (12).

Note that the resulting amplification matrix  $\mathbf{W}_{\text{new}}$  consequently results in  $\mathbf{Q}_{\text{new}}$  as the relay covariance matrix, see (11), and hence belongs to the feasible set of (21b). Moreover, the choice of  $\mathbf{V}$  does not affect the corresponding  $\mathbf{Q}_{\text{new}}$ , and hence does not affect the feasibility. Hence it can be chosen similar to that of  $\mathbf{W}_{\text{old}}$ , with no need for modification in the projection process:

$$\mathbf{V} \leftarrow (\mathbf{Q}_{\text{old}})^{-\frac{1}{2}} \mathbf{W}_{\text{old}} \mathbf{U}_{r,\text{old}} (\mathbf{\Sigma}_{r,\text{old}})^{\frac{1}{2}} \mathbf{U}_{r,\text{old}}^H, \quad (26)$$

where  $\mathbf{U}_{r,\text{old}} \mathbf{\Sigma}_{r,\text{old}} \mathbf{U}_{r,\text{old}}^H$  is the eigenvalue decomposition of  $\mathcal{R}(\mathbf{Q}_{\text{old}})$ .

##### B. Iterative update for $P_s$

For fixed values of  $\mathbf{W}$  and  $\mathbf{z}$ , an increase in  $P_s$  results in an increase in the desired received power, see (18). On the other hand, it also results in an increase in  $P_{\text{err}}$ , due to the direct source-destination interference, as well as the increased received power at the relay which results in an amplified distortion effect. As a result, the impact of the choice of  $P_s$  on the end-to-end SDNR is not clear. The following lemma provides an answer to this question.

**Lemma IV.1.** *For fixed values of  $\mathbf{W}$  and  $\mathbf{z}$  the resulting SDNR is a concave and increasing function of  $P_s$ . Hence, the optimum  $P_s$  is given as*

$$P_s^* = \min \left\{ P_{s,\max}, \tilde{P}_{s,\max}(\mathbf{W}) \right\}, \quad (27)$$

where  $\tilde{P}_{s,\max}(\mathbf{W})$  represents the value of  $P_s$  that results in the maximum relay transmit power, i.e.,  $P_{r,\max}$ , with  $\mathbf{W}$  as the relay amplification matrix.

*Proof:* See Appendix A ■

It is worth mentioning that for a setup with a weak direct link, i.e.,  $\|\mathbf{h}_{sd}\|_2 \approx 0$ , we have  $P_s^* = P_{s,\max}$  for a jointly optimal choice of  $\mathbf{W}, P_s$ . This is grounded on the fact that for any  $P_s < P_{s,\max}$ , the joint variable update  $P_s \leftarrow P_{s,\max}$  and  $\mathbf{W} \leftarrow \mathbf{W} \sqrt{\frac{P_s}{P_{s,\max}}}$ , result in the same  $P_{\text{des}}$ , see (18), while decreasing the  $P_{\text{err}}$ , see (20) in connection to (17).

### C. Iterative update for $\mathbf{z}$

It is apparent that the relay transmit covariance, and hence the constraints in (21b) are invariant to the choice of receive linear filter. The optimal choice of  $\mathbf{z}$  for a given  $\mathbf{W}, P_s$  is obtained as

$$\mathbf{z}^* = \left( \mathbf{H}_{rd}(\mathbf{Q} + \kappa \text{diag}(\mathbf{Q})) \mathbf{H}_{rd}^H + \sigma_{nd}^2 \mathbf{I}_{M_d} + P_s \mathbf{h}_{sd} \mathbf{h}_{sd}^H \right)^{-1} \times \sqrt{P_s} \mathbf{H}_{rd} \mathbf{W} \mathbf{h}_{sr}. \quad (28)$$

The value of  $\mathbf{z}$  is updated according to (28) after the update for  $\mathbf{W}, P_s$ . The update iterations are continued until a stable point is achieved, or a certain number of iterations is expired, see Algorithm 1.

---

**Algorithm 1** Iterative SDNR maximization algorithm based on GP. Number of algorithm iterations are determined by  $c_1 \in \mathbb{R}^+$  and  $C_1 \in \mathbb{N}$ .

---

```

1: Counter  $\leftarrow$  0
2: repeat (running for multiple initializations)
3:   Counter  $\leftarrow$  Counter + 1
4:    $\ell \leftarrow$  0
5:    $P_s^{(0)} \leftarrow P_{s,\max} \times 10^{-4}$ 
6:    $\mathbf{Q}^{(0)} \leftarrow$  random init., see (21b)
7:    $\mathbf{W}^{(0)} \leftarrow \mathbf{Q}^{(0)\frac{1}{2}} \mathcal{R}^{-\frac{1}{2}}(\mathbf{Q}^{(0)})$ , see (25), (12)
8:   repeat
9:      $\ell \leftarrow \ell + 1$ 
10:     $\mathbf{W}^{(\ell)} \leftarrow$  update  $\mathbf{W}^{(\ell)}$ , see (22), (25), Section IV.B
11:     $P_s^{(\ell)} \leftarrow$  update, see (27)
12:     $\mathbf{z}^{(\ell)} \leftarrow$  update, see (28)
13:    SDNR $^{(\ell)} \leftarrow$  (21a)
14:    until SDNR $^{(\ell)} - \text{SDNR}^{(\ell-1)} \geq c_1$  (until SDNR improves)
15:     $\mathcal{A} \leftarrow$  save (SDNR $^{(\ell)}, \mathbf{W}^{(\ell)}, \mathbf{z}^{(\ell)}$ )
16:  until Counter  $\leq C_1$ 
17: return ( $\mathbf{W}, \mathbf{z}, \text{SDNR}$ )  $\leftarrow$  max SDNR  $\in \mathcal{A}$ 

```

---

## V. AN INTUITIVE APPROACH: DISTORTION-AWARE MULTI-STAGE RANK-1 RELAY AMPLIFICATION (MUSTR1)

The proposed method in Section IV directly deals with the SDNR as optimization objective, which also leads to the maximization of end-to-end mutual information for Gaussian signal codewords. Nevertheless, the proposed procedure imposes a high computational complexity, due to the number of the required iterations. In this section we introduce a simpler design by considering a rank-one relay amplification matrix. Note that the near-optimality of rank-one relay amplification matrices for single stream communication has been established, see the arguments in [31, Subsection 3.2] and [30, Section III]. Nevertheless, in the aforementioned works, the impacts of

transmit/receive distortion have not been considered in the FD transceiver. A rank-one relay amplification process is expressed as

$$\mathbf{W} = \sqrt{\omega} \mathbf{w}_{\text{tx}} \mathbf{w}_{\text{tx}}^H, \quad (32)$$

where  $\mathbf{w}_{\text{tx}} \in \mathbb{C}^{M_r}$ ,  $\|\mathbf{w}_{\text{tx}}\|_2 = 1$  and  $\mathbf{w}_{\text{rx}} \in \mathbb{C}^{M_t}$ ,  $\|\mathbf{w}_{\text{rx}}\|_2 = 1$ , respectively act as the receive and transmit linear filters at the relay, while  $\omega \in \mathbb{R}^+$  acts as a scaling factor, see Fig. 2. The idea is to separately design the transmit (receive) filters to maximize the SDNR at each segment. Afterwards, the value of  $\omega$  is optimized. A detailed role and design strategy for the aforementioned parts is elaborated in the following.

### A. Design of $\mathbf{w}_{\text{tx}}$

The role of  $\mathbf{w}_{\text{tx}}$  is to direct the relay transmit beam towards the destination, while imposing minimal distortion on the receiver end of the relay and destination nodes. For this purpose we define the following optimization problem

$$\max_{\mathbf{w}_{\text{tx}}, \|\mathbf{w}_{\text{tx}}\|_2=1} \frac{\mathbb{E}\{\|\mathbf{H}_{rd} \mathbf{u}_{\text{out}}\|_2^2\}}{\mathbb{E}\{\|\mathbf{H}_{D,\text{tx}} \mathbf{u}_{\text{out}}\|_2^2\} + \text{tr}(P_s \mathbf{h}_{sd} \mathbf{h}_{sd}^H + \sigma_{nd}^2 \mathbf{I}_{M_d})}, \quad (33)$$

where the nominator is the desired received power from the relay-destination path, and  $\mathbf{H}_{D,\text{tx}}$  is the equivalent distortion channel observed from the relay transmitter, see Appendix B. The optimization problem (33) can be hence formulated as<sup>3</sup>

$$\max_{\mathbf{w}_{\text{tx}}, \|\mathbf{w}_{\text{tx}}\|_2=1} \frac{\mathbf{w}_{\text{tx}}^H (\mathbf{H}_{rd}^H \mathbf{H}_{rd}) \mathbf{w}_{\text{tx}}}{\mathbf{w}_{\text{tx}}^H (\mathbf{H}_{D,\text{tx}}^H \mathbf{H}_{D,\text{tx}} + N_{\text{tx}} \mathbf{I}_{M_t}) \mathbf{w}_{\text{tx}}}, \quad (34)$$

which holds a generalized Rayleigh quotient structure [44], and  $N_{\text{tx}} := (M_d \sigma_{nd}^2 + P_s \|\mathbf{h}_{sd}\|_2^2) / P_{r,\max}$ . The optimal transmit filter is hence obtained as

$$\mathbf{w}_{\text{tx}}^* := \lambda_{\max} \left\{ (\mathbf{H}_{D,\text{tx}}^H \mathbf{H}_{D,\text{tx}} + N_{\text{tx}} \mathbf{I}_{M_t})^{-1} (\mathbf{H}_{rd}^H \mathbf{H}_{rd}) \right\}. \quad (35)$$

### B. Design of $\mathbf{w}_{\text{rx}}$

The role of  $\mathbf{w}_{\text{rx}}$ , is to accept the desired received signal from the source, while rejecting the received distortion-plus-noise terms at the relay. Similar to (33) this is expressed as

$$\max_{\mathbf{w}_{\text{rx}}} \frac{\mathbf{w}_{\text{rx}}^H (\mathbf{h}_{sr} \mathbf{h}_{sr}^H) \mathbf{w}_{\text{rx}}}{\mathbf{w}_{\text{rx}}^H (\mathbf{\Phi} + \sigma_{nr}^2 \mathbf{I}_{M_r}) \mathbf{w}_{\text{rx}}}, \quad \text{s.t. } \|\mathbf{w}_{\text{rx}}\|_2 = 1, \quad (36)$$

where

$$\mathbf{\Phi} = \kappa P_{r,\max} \mathbf{H}_{\text{tr}} \text{diag}(\mathbf{w}_{\text{tx}} \mathbf{w}_{\text{tx}}^H) \mathbf{H}_{\text{tr}}^H + \beta P_{r,\max} \text{diag}(\mathbf{H}_{\text{tr}} \mathbf{w}_{\text{tx}} \mathbf{w}_{\text{tx}}^H \mathbf{H}_{\text{tr}}^H) \quad (37)$$

approximates the covariance of the received distortion signal at the relay. The optimal solution to  $\mathbf{w}_{\text{rx}}$  can be hence obtained as

$$\mathbf{w}_{\text{rx}}^* := \lambda_{\max} \left\{ (\mathbf{\Phi} + \sigma_{nr}^2 \mathbf{I}_{M_r})^{-1} (\mathbf{h}_{sr} \mathbf{h}_{sr}^H) \right\}. \quad (38)$$

---

<sup>3</sup>For the calculation of the spatial filters  $\mathbf{w}_{\text{tx}}$  and  $\mathbf{w}_{\text{rx}}$ , it is assumed that the relay operates with maximum power, to emphasize the impact of hardware distortions. The relay transmit power is afterwards adjusted by the choice of  $\omega$ . An alternating adjustment of the spatial filters with the optimized relay power is later discussed in Subsection V-E.

$$\begin{aligned} \text{vec}(\nabla P_{\text{err}})^T &= \text{vec} \left( (\mathbf{H}_{\text{rd}}^H \mathbf{z} \mathbf{z}^H \mathbf{H}_{\text{rd}})^T \right)^T \left( \mathbf{I}_{M_t^2} + \kappa \mathbf{S}_D^{M_t} \right) \left( \left[ \mathbf{c} + \mathbf{C}(\mathbf{I}_{M_t^2} - (\mathbf{W}^* \otimes \mathbf{W}) \mathbf{C})^{-1} (\mathbf{W}^* \otimes \mathbf{W}) \mathbf{c} \right]^T \right. \\ &\quad \left. \otimes (\mathbf{I}_{M_t^2} - (\mathbf{W}^* \otimes \mathbf{W}) \mathbf{C})^{-1} \right) \mathbf{S}_K (\mathbf{w} \otimes \mathbf{I}_{M_r M_t}) - (\mathbf{z}^T \mathbf{H}_{\text{rd}}^*) \otimes (P_s \mathbf{z}^H \mathbf{H}_{\text{rd}} \mathbf{W} \mathbf{h}_{\text{sr}} \mathbf{h}_{\text{sr}}^H) \mathbf{S}_T, \end{aligned} \quad (29)$$

$$\text{vec}(\nabla P_{\text{des}})^T = (\mathbf{z}^T \mathbf{H}_{\text{rd}}^*) \otimes (P_s \mathbf{z}^H \mathbf{H}_{\text{rd}} \mathbf{W} \mathbf{h}_{\text{sr}} \mathbf{h}_{\text{sr}}^H) \mathbf{S}_T, \text{ where } \mathbf{w} := \text{vec}(\mathbf{W}), \mathbf{S}_K \in \{0, 1\}^{M_r^2 M_t^2 \times M_r^2 M_t^2}, \mathbf{S}_T \in \{0, 1\}^{M_r M_t \times M_r M_t}, \quad (30)$$

$$\text{such that: } \text{vec}(\mathbf{W}^* \otimes \mathbf{W}) = \mathbf{S}_K \text{vec}(\mathbf{w}^* \mathbf{w}^T), \text{ and } \mathbf{S}_T \text{vec}(\mathbf{W}) = \text{vec}(\mathbf{W}^T). \quad (31)$$

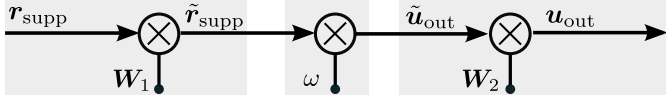


Figure 2. The relay amplification is divided into three parts:  $\mathbf{w}_{\text{rx}}$  and  $\mathbf{w}_{\text{tx}}$  respectively represent the reception and transmit filters, and  $\omega$  represents the scaling factor. The bold arrows represent the vector signals while the dashed arrows represent the scalars. The overall process can be described as  $\mathbf{W} = \omega \mathbf{w}_{\text{tx}} \mathbf{w}_{\text{rx}}^H$ .

### C. Design of $\omega$

The role of  $\omega$  is to adjust the amplification intensity at the relay. This plays a significant role, considering the fact that even with optimally designed spatial filters, i.e.,  $\mathbf{w}_{\text{rx}}$  and  $\mathbf{w}_{\text{tx}}$ , a weak amplification at the relay reduces the desired signal strength at the destination, resulting to a low signal-to-noise ratio. On the other hand, a strong amplification may lead to instability and (theoretically) infinite distortion transmit power, i.e., low signal-to-distortion ratio. Hence, similar to (21), we focus on maximizing the end-to-end SDNR, assuming that  $\mathbf{w}_{\text{rx}}$  and  $\mathbf{w}_{\text{tx}}$  are given from the previous parts. The end-to-end SDNR and the transmit power from the relay corresponding to a value of  $\omega$  are respectively approximated as  $f_1$  and  $f_2$  such that

$$f_1(\omega) = a_d \omega \left( a_0 + \sum_{k \in \mathbb{F}_K} a_k \omega^k \right)^{-1}, \quad (39)$$

and

$$f_2(\omega) = \sum_{k \in \mathbb{F}_K} b_k \omega^k, \quad (40)$$

where

$$a_d = P_s \mathbf{d}_{M_d}^T (\mathbf{H}_{\text{rd}}^* \otimes \mathbf{H}_{\text{rd}}) \tilde{\mathbf{W}} \text{vec}(\mathbf{h}_{\text{sr}} \mathbf{h}_{\text{sr}}^H), \quad (41)$$

$$a_0 = \mathbf{d}_{M_d}^T \text{vec}(\sigma_{\text{nd}}^2 \mathbf{I}_{M_d} + P_s \mathbf{h}_{\text{sd}} \mathbf{h}_{\text{sd}}^H), \quad (42)$$

$$a_1 = -a_d + \mathbf{d}_{M_d}^T (\mathbf{H}_{\text{rd}}^* \otimes \mathbf{H}_{\text{rd}}) (\mathbf{I}_{M_t^2} + \kappa \mathbf{S}_D^{M_t}) \tilde{\mathbf{W}} \mathbf{c}, \quad (43)$$

$$a_k = \mathbf{d}_{M_d}^T (\mathbf{H}_{\text{rd}}^* \otimes \mathbf{H}_{\text{rd}}) (\mathbf{I}_{M_t^2} + \kappa \mathbf{S}_D^{M_t}) \times (\tilde{\mathbf{W}} \mathbf{C})^{k-1} \tilde{\mathbf{W}} \mathbf{c}, \quad k \in \{2 \dots K\}, \quad (44)$$

$$b_k = \mathbf{d}_{M_t}^T (\mathbf{I}_{M_t^2} + \kappa \mathbf{S}_D^{M_t}) (\tilde{\mathbf{W}} \mathbf{C})^{k-1} \tilde{\mathbf{W}} \mathbf{c}, \quad k \in \mathbb{F}_K, \quad (45)$$

see Appendix C for more details. In the above expressions  $K$  is the approximation order and  $\mathbf{d}_M \in \{0, 1\}^{M^2}$  is defined such that  $\text{tr}(\mathbf{A}) = \mathbf{d}_M^T \text{vec}(\mathbf{A})$ ,  $\mathbf{A} \in \mathbb{C}^{M \times M}$ . Furthermore  $\mathbf{C}$ ,  $\mathbf{c}$ ,  $\tilde{\mathbf{W}}$  are respectively defined in (15), (16) and in Appendix C. The corresponding optimization problem can be written as

$$\max_{\omega} f_1(\omega) \quad (46a)$$

$$\text{s.t. } 0 \leq \omega \leq \min\{\omega_{\text{infty}}, \omega_{\text{max}}\} = \omega_{\text{max}}, \quad (46b)$$

where  $\omega_{\text{max}}$  corresponds to the relay amplification that results in a tight transmit power constraint, i.e.,  $f_2(\omega_{\text{max}}) = P_{\text{r,max}}$ . Moreover,  $\omega_{\text{infty}}$  is the smallest pole of  $f_2(\omega)$  in the real positive domain which yields to the instability of the relay distortion loop, i.e., infinite relay transmit power. We observe that while  $f_1(\omega)$  remains positive and differentiable in the domain  $[0, \omega_{\text{infty}})$ , we have  $f_1(\omega) \rightarrow 0$  and  $f_1'(\omega) \rightarrow 0$ .

This concludes the existence of (at least) one local maximum point in this domain, see Fig. 3 for a visual description. By setting the derivative of (39) to zero, we conclude that the resulting extremum points are necessarily located such that

$$a_0 = \sum_{k \in \mathbb{F}_K} (k-1) a_k \omega^k. \quad (47)$$

While the left side of (47) is a constant, the right side of the equality is monotonically increasing with respect to  $\omega \in \mathbb{R}^+$ , as  $a_k \geq 0, \forall k$ . This readily results in the exactly one extremum point in the positive domain of  $\omega^4$ . Hence, the optimality occurs either at the obtained extremum point, i.e., a local maximum in the domain  $[0, \omega_{\text{max}})$ , see Fig. 3-a, or at the point where the relay transmit power constraint is tight, see Fig. 3-b. The optimum  $\omega$  can be hence formulated as

$$\omega^* = \min\{\omega_0, \omega_{\text{max}}\}, \quad (48)$$

where  $\omega_0$  is the only solution of (47) in the positive domain.

### D. Design of $\mathbf{z}$

The optimal design of  $\mathbf{z}$  is given in (28) as a closed form expression. Note that the solution of  $\mathbf{z}$  is dependent on the choice of other optimization variables. However, as the

<sup>4</sup>Note that both  $f_2(\omega_{\text{max}}) = P_{\text{r,max}}$  or (47) result in exactly one solution for  $\omega$  in  $\mathbb{R}^+$ , as  $a_k, b_k \geq 0, \forall k$ . In this regard, values of  $\omega_{\text{max}}$  and  $\omega_0$  can be obtained via a bi-section search, or can be obtained in closed-form for small values of  $K$ , i.e.,  $K \leq 3$ , as a known polynomial root.

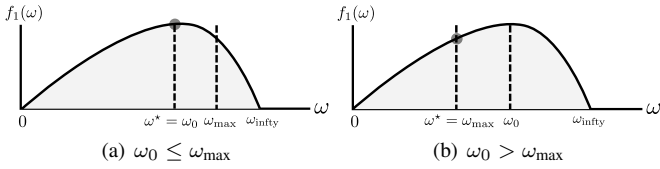


Figure 3. Possible situations of  $\omega_0$  with respect to  $\omega_{\max}$ , considering the feasible region of  $\omega$ . The dark circle indicates the position of the optimum point.

proposed designs for the other optimization variables do not depend on  $\mathbf{z}$ , there is no need for further alternation among the design parameters. The Algorithm 2 defines the required steps.

**Algorithm 2** Distortion Aware Multi-Stage Rank-1 Relay amplification (MuStR1) for SDNR maximization. The solution is obtained with no alternation among the optimization variables.

- 
- 1:  $P_s \leftarrow P_{s,\max}$
  - 2:  $\mathbf{w}_{\text{tx}} \leftarrow$  calculate Tx filter, see (35)
  - 3:  $\mathbf{w}_{\text{rx}} \leftarrow$  calculate Rx filter, see (38)
  - 4:  $\omega \leftarrow$  adjust amplification intensity, see Subsection V-C
  - 5:  $\mathbf{z} \leftarrow$  see (28)
  - 6: **return** ( $\mathbf{z}$ ,  $\mathbf{W} = \omega \mathbf{w}_{\text{tx}} \mathbf{w}_{\text{rx}}^H$ )
- 

#### E. Alternating enhancement of MuStR1 (AltMuStR1)

The proposed MuStR1 design is accomplished with no alternation among the optimization variables, see Algorithm 2. In this part we provide an alternating enhancement of MuStR1 which results in an increased performance, at the expense of a higher computational complexity. In order to accomplish this purpose, similar to (18) and (20) we focus on the signal and power values at the destination, after the application of  $\mathbf{z}$ . In this respect, the values of  $\mathbf{w}_{\text{tx}}$ ,  $\mathbf{w}_{\text{rx}}$ ,  $\mathbf{z}$  and  $\omega$  will be calculated as a joint alternating optimization. This is done by replacing  $\mathbf{H}_{\text{rd}}$  with  $\mathbf{z}^H \mathbf{H}_{\text{rd}}$  in the design of  $\mathbf{w}_{\text{tx}}$ , and  $\mathbf{d}^T$  with  $(\mathbf{z}^T \otimes \mathbf{z}^H)$  in (41)-(44). The steps 2-6 in Algorithm 2 are then repeated until a stable point is achieved. The performance of the proposed (Alt)MuStR1 algorithms in terms of the resulting communication rate, convergence, and computational complexity are studied via numerical simulations in Subsection VII-A. In particular, it is observed that the performance of the AltMuStR1 algorithm reaches close to the performance of GP, with a significantly lower computational complexity.

## VI. COMPARISON WITH DECODE-AND-FORWARD RELAYING UNDER RESIDUAL SELF-INTERFERENCE

In the previous sections we studied the behavior of an AF-FD relay under residual self-interference, from the aspects of performance analysis and design methodologies. While an AF relaying is known to provide a simple strategy, it particularly suffers from the aforementioned distortion loop especially when the residual interference power is not ignorable, see Subsection II-D. In this part, we provide a similar study for a setup where the relay operates with DF protocol, in order to act as a comparison benchmark. In a DF relay, the discussed distortion

loop is significantly alleviated as the decoding process eliminates the inter-dependency of the received residual interference intensity to the relay transmit signal power, see [16, Section V] for a similar discussion regarding single antenna relays. Note that optimization strategies for FD relays with DF process have been discussed in the literature, see [10]–[12], [14], for different relaying setups and assumptions. In order to adopt the available literature to our setup, we follow a modified version of the approach given in [12], [14], where an SDNR maximization problem is studied at a MIMO DF relay. Note that the proposed design in [12], [14] considers a maximization of the SDNR at the relay input/output, taking advantage of spatial and temporal filters. In our system, we focus on the resulting performance from the source to the destination, after the application of the receive filter  $\mathbf{z}$ , and hence including  $P_s$  and  $\mathbf{z}$  as optimization variables. Afterwards, similar to [14], we propose a joint optimization where in each step one of the variables is updated to the optimality. A detailed model update and design strategy is given in the following.

#### A. DF Relaying

We define  $\mathbf{v}_{\text{in}} \in \mathbb{C}^{M_r}$  as linear filter at the relay input,  $\hat{s}_r \in \mathbb{C}$ ,  $\mathbb{E}\{|\hat{s}_r|^2\} = 1$  as the decoded symbol, and  $\mathbf{v}_{\text{out}} \in \mathbb{C}^{M_t}$  as the beamforming vector to transmit the decoded data symbol, see Fig. 4. The end-to-end rate maximization can be equivalently formulated as

$$\begin{aligned} \max_{\mathbf{v}_{\text{in}}, \mathbf{z}, \mathbf{Q} \in \mathcal{H}, P_s} \quad & \min(\zeta_{\text{sr}}, \zeta_{\text{rd}}), \\ \text{s.t.} \quad & \text{tr}(\mathbf{Q}) \leq \tilde{P}_{r,\max}, P_s \leq P_{s,\max}, \text{rank}(\mathbf{Q}) = 1, \end{aligned} \quad (49a)$$

$$(49b)$$

where the rank-one constraint is imposed to ensure the structure  $\mathbf{Q} := \mathbb{E}\{\mathbf{u}_{\text{out}} \mathbf{u}_{\text{out}}^H\} = \mathbf{v}_{\text{out}} \mathbf{v}_{\text{out}}^H$ . The values  $\zeta_{\text{sr}}$  and  $\zeta_{\text{rd}}$ , respectively represent the resulting SDNR in source-to-relay and relay-to destination links which can be calculated as

$$\zeta_{\text{sr}} \approx \frac{P_s \mathbf{v}_{\text{in}}^H \mathbf{h}_{\text{sr}} \mathbf{h}_{\text{sr}}^H \mathbf{v}_{\text{in}}}{\mathbf{v}_{\text{in}}^H \left( \sigma_{\text{nr}}^2 \mathbf{I}_{M_r} + \kappa \mathbf{H}_{\text{rr}} \text{diag}(\mathbf{Q}) \mathbf{H}_{\text{rr}}^H + \beta \text{diag}(\mathbf{H}_{\text{tr}} \mathbf{Q} \mathbf{H}_{\text{tr}}^H) \right) \mathbf{v}_{\text{in}}}, \quad (50)$$

$$\zeta_{\text{rd}} = \frac{\mathbf{z}^H \mathbf{H}_{\text{rd}} \mathbf{Q} \mathbf{H}_{\text{rd}}^H \mathbf{z}}{\mathbf{z}^H \left( \sigma_{\text{nd}}^2 \mathbf{I}_{M_d} + \kappa \mathbf{H}_{\text{rd}} \text{diag}(\mathbf{Q}) \mathbf{H}_{\text{rd}}^H + P_s \mathbf{h}_{\text{sd}} \mathbf{h}_{\text{sd}}^H \right) \mathbf{z}}. \quad (51)$$

where the approximation in (50) follows considering the fact that the self-interference signal constitutes the dominant part of the power in  $\mathbf{u}_{\text{in}}$ , and can be regarded as the only cause of distortion signals at the relay, see also (9). Note that (49) is not a convex optimization problem, and also can not be solved in a closed form. Nevertheless, recognizing the generalized Rayleigh quotient structure in (50), (51) we obtain

$$\mathbf{z}^* = \left( \sigma_{\text{nd}}^2 \mathbf{I}_{M_d} + \kappa \mathbf{H}_{\text{rd}} \text{diag}(\mathbf{Q}) \mathbf{H}_{\text{rd}}^H + P_s \mathbf{h}_{\text{sd}} \mathbf{h}_{\text{sd}}^H \right)^{-1} \mathbf{H}_{\text{rd}} \mathbf{v}_{\text{out}}, \quad (52)$$

$$\mathbf{v}_{\text{in}}^* = \left( \sigma_{\text{nr}}^2 \mathbf{I}_{M_r} + \kappa \mathbf{H}_{\text{rr}} \text{diag}(\mathbf{Q}) \mathbf{H}_{\text{rr}}^H + \beta \text{diag}(\mathbf{H}_{\text{tr}} \mathbf{Q} \mathbf{H}_{\text{tr}}^H) \right)^{-1} \times \mathbf{h}_{\text{sr}} \sqrt{P_s}, \quad (53)$$

where  $\mathbf{z}^*$ ,  $\mathbf{v}_{\text{in}}^*$  represent the optimum  $\mathbf{z}$ ,  $\mathbf{v}_{\text{in}}$  for a fixed  $\mathbf{Q}$  and  $P_s$ . In order to obtain the optimal  $\mathbf{Q}$ ,  $P_s$ , the problem in (49) can be re-formulated as

$$\max_{P_s, \zeta \in \mathbb{R}^+, \mathbf{Q} \in \mathcal{H}} \zeta \quad (54a)$$

$$\text{s.t.} \quad \zeta \leq \zeta_{\text{sr}}, \quad \zeta \leq \zeta_{\text{rd}}, \quad (54b)$$

$$\mathbf{Q} \in \mathcal{H}, \quad \text{tr}(\mathbf{Q}) \leq \tilde{P}_{r, \text{max}}, \quad \text{rank}(\mathbf{Q}) = 1, \quad (54c)$$

where the values of  $\mathbf{v}_{\text{in}}$  and  $\mathbf{z}$  are fixed. By temporarily relaxing the rank constraint, the above problem can be written as a convex feasibility check over  $\mathbf{Q}$ ,  $P_s$ , for each value of  $\zeta$  as

$$\text{find } \mathbf{Q}, P_s \quad (55a)$$

$$\text{s.t.} \quad \text{tr}(\mathbf{Q}) \leq \tilde{P}_{r, \text{max}}, \quad P_s \geq 0, \quad \mathbf{Q} \in \mathcal{H}, \quad (55b)$$

$$\text{tr}(\Psi_{\text{sr}} + \Phi_{\text{sr}} \mathbf{Q}) \geq 0, \quad \text{tr}(\Psi_{\text{rd}} + \Phi_{\text{rd}} \mathbf{Q}) \geq 0, \quad (55c)$$

where

$$\Psi_{\text{rd}} := -\zeta \mathbf{z} \mathbf{z}^H (\sigma_{\text{nd}}^2 \mathbf{I}_{M_d} + P_s \mathbf{h}_{\text{sd}} \mathbf{h}_{\text{sd}}^H) \quad (56)$$

$$\Psi_{\text{sr}} := \mathbf{v}_{\text{in}} \mathbf{v}_{\text{in}}^H (P_s \mathbf{h}_{\text{sr}} \mathbf{h}_{\text{sr}}^H - \zeta \sigma_{\text{nr}}^2 \mathbf{I}_{M_r}), \quad (57)$$

$$\Phi_{\text{rd}} := \mathbf{H}_{\text{rd}}^H \mathbf{z} \mathbf{z}^H \mathbf{H}_{\text{rd}} - \zeta \kappa \text{diag}(\mathbf{H}_{\text{rd}}^H \mathbf{z} \mathbf{z}^H \mathbf{H}_{\text{rd}}), \quad (58)$$

$$\Phi_{\text{sr}} := -\zeta (\kappa \text{diag}(\mathbf{H}_{\text{tr}}^H \mathbf{v}_{\text{in}} \mathbf{v}_{\text{in}}^H \mathbf{H}_{\text{tr}}) + \beta \mathbf{H}_{\text{tr}}^H \text{diag}(\mathbf{v}_{\text{in}} \mathbf{v}_{\text{in}}^H) \mathbf{H}_{\text{tr}}). \quad (59)$$

Note that the iterations of the defined feasibility check will be continued, following a bi-section search procedure until an optimum  $\zeta$  is obtained with sufficient accuracy. Fortunately, for the special structure of (55) as a complex-valued semi-definite program with three linear constraints, we can always achieve an optimal rank-1  $\mathbf{Q} \in \mathcal{H}$ , following [45, Theorem 3.2]. The optimal  $\mathbf{v}_{\text{in}}$  is hence obtained as

$$\mathbf{v}_{\text{out}}^* = \mathbf{Q}^{\frac{1}{2}}, \quad (60)$$

where  $\mathbf{Q}^*$  represents the obtained  $\mathbf{Q}$  for the highest feasible  $\zeta$ . It is worth mentioning that the feasible values of  $\zeta$  is necessarily located in the region  $[0, \zeta_{\text{max}}]$  where

$$\zeta_{\text{max}} := \min \left\{ \frac{P_{s, \text{max}} \|\mathbf{h}_{\text{sr}}\|_2^2}{\sigma_{\text{nr}}^2}, \frac{P_{r, \text{max}} \lambda_{\text{max}}\{\mathbf{H}_{\text{rd}} \mathbf{H}_{\text{rd}}^H\}}{\sigma_{\text{nd}}^2} \right\} \quad (61)$$

corresponds to the minimum of the individual link qualities, assuming  $\beta = \kappa = 0$ , and will be used as the initial bounds for the aforementioned bi-section search. The iterations of the defined optimization steps is continued until a stable point is obtained, or a pre-defined number of iterations is expired. Note that the solutions in (52)-(60), result in a necessary improvement of  $\zeta$ , since in each step the defined sub-problem is solved to optimality. Moreover, since the performance of the studied relay system is bounded from above, see (61), the defined iterative update results in a necessary convergence. Algorithm 3 provides a detailed procedure.

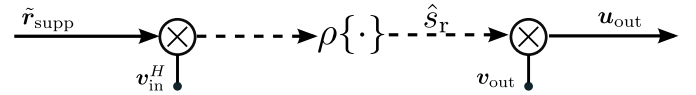


Figure 4. A schematic of a decode-and-forward relaying process.  $\rho\{\cdot\}$  and  $\hat{s}_r$  represent the decoding process, and the estimate of the transmitted symbol,  $s$ , at the relay. The receive and transmit spatial filters are represented as  $\mathbf{v}_{\text{in}}$  and  $\mathbf{v}_{\text{out}}$ , respectively. The bold arrows represent the vector signals while the dashed arrows represent the scalars.

**Algorithm 3** An iterative rate maximization algorithm for decode-and-forward relaying.  $C_1, C_2 \in \mathbb{N}$  respectively represent the number of the main optimization steps and the bi-section process, and  $c_1 \in \mathbb{R}^+$  determines the stability condition.

---

```

1:  $P_s \leftarrow P_{s, \text{max}} \times 10^{-2}$ 
2:  $\text{counter}_1 \leftarrow 0$ 
3: repeat (main optimization steps)
4:    $\text{counter}_1 \leftarrow \text{counter}_1 + 1$ 
5:    $\mathbf{v}_{\text{in}} \leftarrow \mathbf{v}_{\text{in}}^*$ , see (53)
6:    $\mathbf{z} \leftarrow \mathbf{z}^*$ , see (52)
7:    $\text{counter}_2 \leftarrow 0$ 
8:    $\zeta_{\text{min}} \leftarrow 0$ 
9:    $\zeta_{\text{max}} \leftarrow$  see (61)
10:  repeat (bi-section search steps)
11:     $\zeta \leftarrow (\zeta_{\text{min}} + \zeta_{\text{max}})/2$ 
12:    if (55a)-(55b) is feasible then
13:       $\zeta_{\text{min}} \leftarrow \zeta$ 
14:    else
15:       $\zeta_{\text{max}} \leftarrow \zeta$ 
16:    end if
17:  until  $\text{counter}_2 \leq C_2$ 
18:   $\zeta^{\text{counter}_1} \leftarrow (\zeta_{\text{min}} + \zeta_{\text{max}})/2$ 
19:   $P_s \leftarrow P_s^*$ , see (54)
20:   $\mathbf{v}_{\text{out}} \leftarrow \mathbf{v}_{\text{out}}^*$ , see (60)
21: until  $\text{counter}_1 \leq C_1$  or  $\zeta^{\text{counter}_1} - \zeta^{\text{counter}_1 - 1} \leq c_1$ 
22: return  $(P_s, \mathbf{z}, \mathbf{v}_{\text{in}}, \mathbf{v}_{\text{out}})$ 

```

---

## VII. SIMULATION RESULTS

In this section we evaluate the behavior of the studied FD AF relaying setup via numerical simulations. In particular, we evaluate the proposed GP design in Section IV, as well as the (Alt)MuStR1 algorithms in Section V, under the impact of hardware inaccuracies, in comparison with the available relevant methods in the literature. We assume that  $\mathbf{h}_{\text{sr}}$ ,  $\mathbf{H}_{\text{rd}}$  and  $\mathbf{h}_{\text{sd}}$  follow an uncorrelated Rayleigh flat-fading model, where  $\rho_{\text{sr}}$ ,  $\rho_{\text{rd}}$  and  $\rho_{\text{sd}} \in \mathbb{R}^+$  represent the path loss. For the self-interference channel, we follow the characterization reported in [21]. In this respect we have  $\mathbf{H}_{\text{tr}} \sim \mathcal{CN} \left( \sqrt{\frac{\rho_{\text{tr}} K_R}{1 + K_R}} \mathbf{H}_0, \frac{1}{1 + K_R} \mathbf{I}_{M_t} \otimes \mathbf{I}_{M_r} \right)$  where  $\rho_{\text{tr}}$  represents the self-interference channel strength,  $\mathbf{H}_0$  is a deterministic term<sup>5</sup> and  $K_R$  is the Rician coefficient. For each channel realization the resulting performance in terms of the communication rate, i.e.,  $\log_2(1 + \text{SDNR})$ , is evaluated by employing different design strategies and for various system parameters. The overall system performance is then averaged over 500 channel

<sup>5</sup>For simplicity, we choose  $\mathbf{H}_0$  as a matrix of all-1 elements.

Table I. DEFAULT SETUP PARAMETERS

Parameter	$P_{\max} := P_{s,\max} = P_{r,\max}$	$\sigma_n^2 := \sigma_{nr}^2 = \sigma_{nd}^2$	$\kappa = \beta$	$M := M_t = M_r = M_d$	$\rho_{rr}$	$\rho_{sr} = \rho_{rd}$	$\rho_{sd}$	$K_R$
Value	1	-40 [dB]	-40 [dB]	4	1	-30 [dB]	-60 [dB]	10

realizations. Unless explicitly stated, the defined parameters in Table I are used as our default setup.

#### A. Algorithm analysis

In this subsection we study the behavior of the proposed iterative algorithms, i.e., GP and (Alt)MuStR1, in terms of the convergence speed, approximation accuracy, and computational complexity. Moreover, we study the gap of the proposed GP method with the optimality, with the help of an extensive numerical simulation.

1) *Convergence*: Both GP and AltMuStR1 operate based on iterative update of the variables, until a stable point is obtained. A study on the convergence behavior of these algorithms are necessary, in order to verify the algorithm function, and also as a measure of the required computational effort.

In Fig. 5-(a) the average convergence behavior of the GP algorithm is depicted. At each iteration, the obtained performance is depicted as a percentage of the final performance after convergence, where  $\text{SDNR}^*$  is the SDNR at the convergence. It is observed that the convergence speed differs, for different values of transceiver inaccuracy. This is expected, as a higher distortion results in the complication of the mathematical structure by signifying non-quadratic terms, see (17), and requires the application of the projection procedure (Subsection IV-A2) more often. It is observed from our simulations that the algorithm requires  $10^2$  to  $10^4$  number of iterations to converge, depending on the value of the distortion coefficients  $\kappa, \beta$ .

In Fig. 5-(b) the average convergence behavior of the proposed AltMuStR1 is depicted. Note that unlike GP, AltMuStR1 operates based on the local increase of SDNR in the defined relaying segments, see Section V. Hence, a theoretical guarantee on the monotonic increase of the overall SDNR in each iteration is not available. Nevertheless, the numerical evaluation shows that the algorithm converges within much fewer number of iterations, with an effective increase in each step. Similar to GP, a higher value of  $\kappa, \beta$  results in a slower convergence.

2) *Approximation accuracy*: The proposed (Alt)MuStR1 algorithms are based on the used approximation (44) and (45). In this regard, the choice of the approximation order  $K$  leads to a trade-off between algorithm complexity and the resulting performance. In Fig. 6 the exact, and approximated SDNR values are depicted for a pessimistic case of  $\kappa = 0.1$ . By repeating such experiments, we have decided on  $K = 5$  as a good balance between approximation accuracy and the resulting complexity.

3) *GP optimality gap*: Via the application of the gradient ascend the proposed GP converges with a monotonically increasing objective. Nevertheless, the global optimality of the resulting stationary point may not be guaranteed, due to the possibility of a local extrema. In Fig. 7 the performance of GP algorithm is evaluated with multiple random initializations,

where the best converging point is considered as the algorithm solution. It is observed that the occurrence of a local optimum is more likely for higher values of  $\kappa, \beta$ , as a larger number of initial points results in a better performance. Nevertheless, it is observed that no significant performance improvement is observed by employing more than  $C_1 = 10$  number of random initial points. We consider the obtained performance of the GP algorithm with  $C_1 = 10$  as our performance benchmark for FD AF relaying hereinafter.

4) *Computational complexity*: Other than the required number of iterations, the computational demand of an algorithm is impacted by the required per-iteration complexity. In Fig. 5-(c), the required CPU time of the proposed algorithms are depicted as the number of antennas increase. The reported CPU time is obtained using an Intel Core i5 – 3320M processor with the clock rate of 2.6 GHz and 8 GB of random-access memory (RAM). As our software platform we have used MATLAB 2013a, on a 64-bit operating system. While the GP method is considered as the performance benchmark, the proposed (Alt)MuStR1 algorithms show a significant advantage to the GP algorithm in terms of computational complexity.

#### B. Performance comparison

In this part we evaluate the performance of the proposed designs, in comparison with the available designs in the literature.

1) *Available design approaches*: We divide the relevant available literature on the FD AF relaying design into three approaches. Firstly, as considered in [22], [23], the SIC is purely relegated to the relay receiver end, via a combined time domain analog/digital cancellation techniques. The aforementioned approach imposes no design constraint on the self-interference power, i.e.,  $P_{\text{intf}} \leq \infty$ , where  $P_{\text{intf}}$  represents the self-interference power prior to analog/digital cancellation<sup>6</sup>. Secondly, the SIC is purely done via transmit beamforming at the null space of the relay receive antennas, e.g., [25]–[30], hence imposing a zero interference power constraint for transmit beamforming design, i.e.,  $P_{\text{intf}} \leq 0$ . Finally, as a generalization of the aforementioned extreme approaches, a combined transmit beamforming and analog/digital cancellation at the receiver is considered in [31], [32]. In the aforementioned case it is assumed that the received self-interference power should not exceed a certain threshold ( $P_{\text{th}}$ ), i.e.,  $P_{\text{intf}} \leq P_{\text{th}}$ . In all of the aforementioned cases, due to the perfect hardware assumptions, and upon imposition of the required self-interference power constraint, the SIC is assumed to be perfect. In our simulations, we evaluate the generalized approach in [31], [32] by once assuming a high self-interference power threshold, i.e.,  $P_{\text{th}} = P_{r,\max}$ , denoted as

<sup>6</sup>This approach is equivalent to ignoring the impact of SIC in the beamforming design, as it has been usual in the earlier literature.

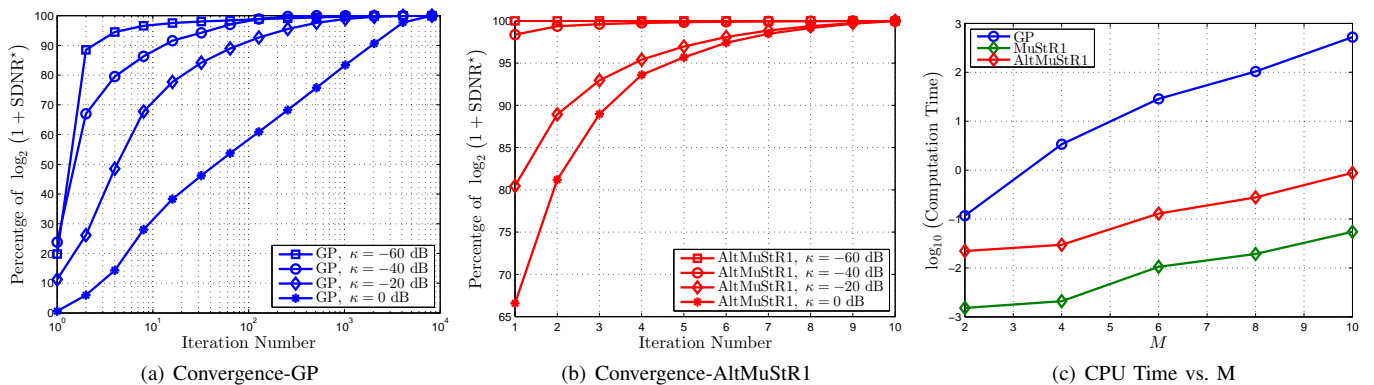


Figure 5. Average convergence behavior of the proposed GP algorithm (a), the AltMuStR1 algorithm (b), and a comparison on computational complexity (c).

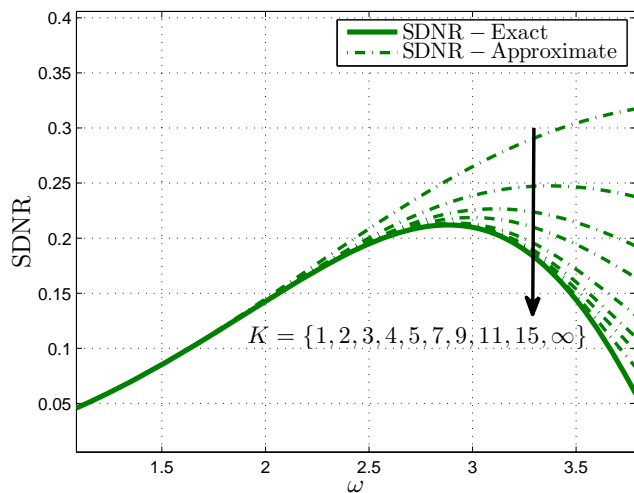


Figure 6. Approximated SDNR value for different approximation orders  $K$ , and  $\kappa = \beta = -10$  dB.

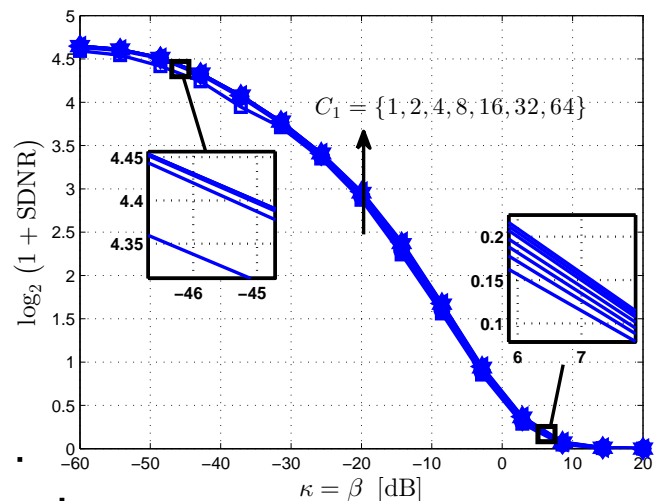


Figure 7. Performance of the proposed GP method for multiple initializations. The resulting performance converges for higher than 8 number of initializations.

' $P_{\text{th-High}}$ ', and once assuming a low self-interference power threshold, i.e.,  $P_{\text{th}} = 0.01 \times P_{\text{r,max}}$ , denoted as ' $P_{\text{th-Low}}$ '<sup>7</sup>.

2) *Decoding gain*: Other than the defined approaches for FD AF relaying, it is interesting to evaluate the impact of decoding in the studied system. This is since in a DF relay, the discussed distortion loop is significantly alleviated as the decoding process eliminates the inter-dependency of the received residual interference intensity to the relay transmit power. In order to adopt the available literature to our setup, we follow a modified version of the approach given in [12], [14], where an SDNR maximization problem is studied at a MIMO DF relay. Please see Section VI for the detailed steps.

<sup>7</sup>Note that the direct application of  $P_{\text{th}} \leq 0$ , and  $P_{\text{th}} \leq \infty$  is not feasible in our scenario. This is since  $P_{\text{th}} \leq 0$  strictly requires that  $M_t > M_r$ , and the  $P_{\text{th}} \leq \infty$  often results in a non-stable relay function due to the impact of the distortion. Nevertheless, the chosen scenarios ' $P_{\text{th-High}}$ ' and ' $P_{\text{th-Low}}$ ' closely capture the nature of the aforementioned designs.

3) *Visualization*: In Figs. 8-13 the average communication rate, i.e.,  $\log_2(1 + \text{SDNR})$ , is evaluated under various system parameters.

In Fig. 8 the impact of the transceiver inaccuracy is depicted. It is observed that as  $\kappa = \beta$  increase, the communication performance decreases for all methods. In this respect, the HD setup remains more robust against the hardware distortions, and outperforms the FD setup for large values of  $\kappa = \beta$ . This is since the strong self-interference channel, as the main cause of distortion, is not present for a HD setup. Relative to the benchmark performance for the FD AF relaying (GP), a significant decoding gain is observed for the big values of  $\kappa$ , where the system performance is dominated by the impact of distortion loop, see Subsection II-D. Moreover, it is observed that the proposed AltMuStR1 method performs close to the GP method for different values of  $\kappa$ . The performance of ' $P_{\text{th-High}}$ ' reaches close to optimality for a small  $\kappa$ , where

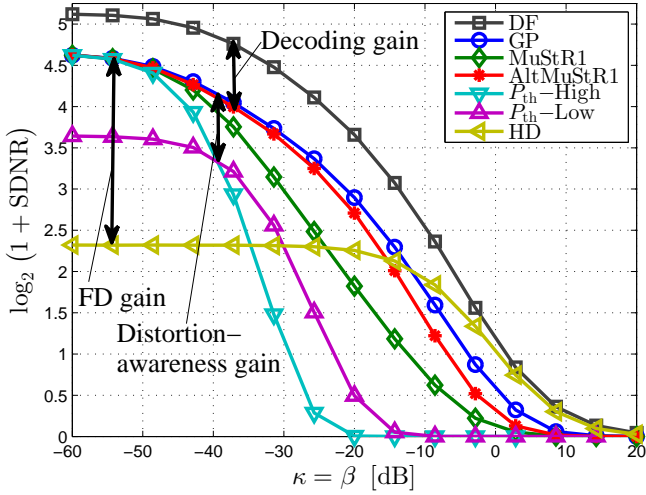


Figure 8. Average communication rate vs. transceiver inaccuracy. The communication rate decreases as the transceiver inaccuracy increases.

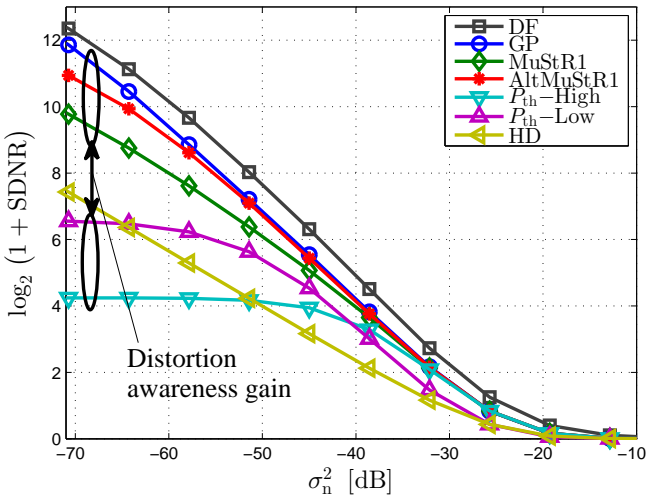


Figure 9. Average communication rate vs. noise variance. The communication rate decreases as the noise variance increases.

the ' $P_{th}$ -Low' reaches a relatively better performance as  $\kappa$  increases. Nevertheless, both of the aforementioned methods degrade rapidly for higher values of  $\kappa$ . This is expected, as the impacts of hardware inaccuracies are not taken into account in the aforementioned approaches.

In Fig. 9 and Fig. 10, the opposite impact of the thermal noise variance,  $\sigma_n^2 = \sigma_{nr}^2 = \sigma_{nd}^2$ , and the maximum transmit power,  $P_{max} = P_{s,max} = P_{r,max}$ , is observed on the average system performance. This is expected, as an increase (decrease) in  $P_{max}$  ( $\sigma_n^2$ ) increases the signal-to-noise ratio, while keeping the signal-to-distortion ratio intact. Furthermore, it is observed that in a low noise (high power) region the performance of the

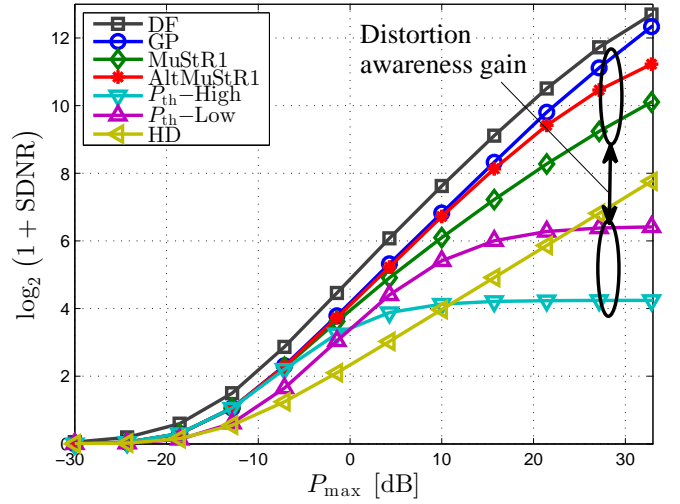


Figure 10. Average communication rate vs. allowed transmit power. A higher transmit power results in a higher communication rate.

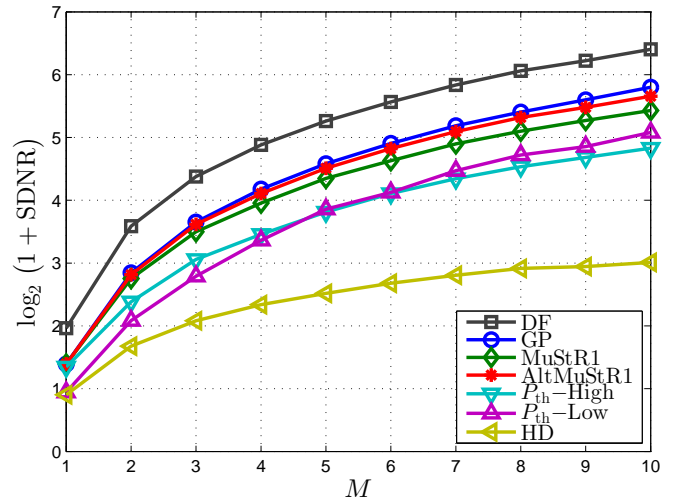


Figure 11. Average communication rate vs. number of antennas. The communication rate increases as the number of antennas increases.

methods with perfect hardware assumptions saturate. This is since the role of hardware distortions become dominant for a high power or a low noise system.

In Fig. 11 the resulting system performance is depicted with respect to the number of antennas. It is observed that the performance of all methods increase as the number of antennas increase. Moreover, the performance of the proposed (Alt)MuStR1 methods remain close to the benchmark GP performance. This is promising, considering the increasing computational complexity of the GP method as the number of antenna increases.

In Fig. 12 the impact of the relay position is observed. In this regard, it is assumed that the source is located with the distance

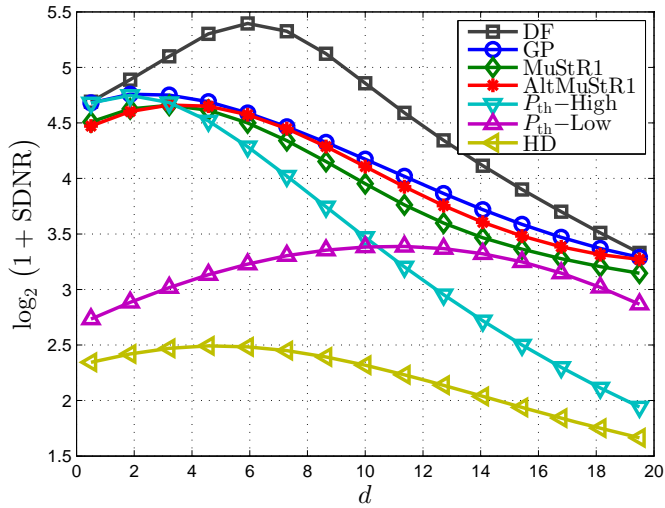


Figure 12. Average communication rate vs. distance of the relay node from the source. The decoding gain is reduced when relay is closed to source or destination.

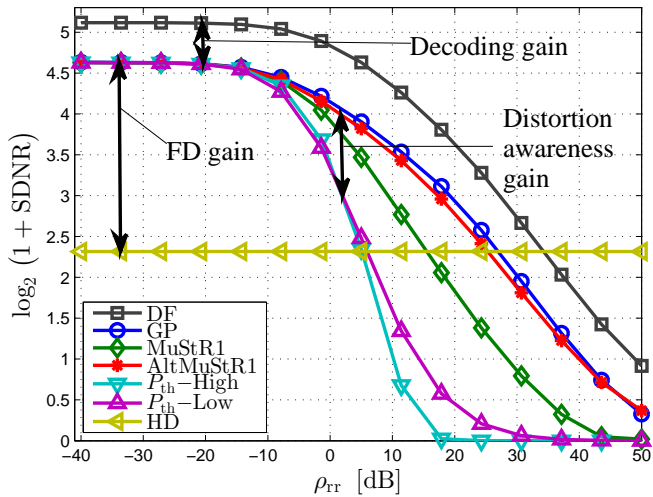


Figure 13. Average communication rate vs. self-interference channel intensity. The communication rate decreases as the self-interference channel intensity increases.

$d_{sr}$  from the relay where the relay is located with the distance  $d_{rd} = 20 - d_{sr}$  from the source. The path loss values for each link is then obtained as  $\rho_X = \frac{0.1}{d^2}$ ,  $X \in \{sr, rd\}$ . As expected, the decoding gain decreases when the relay is positioned close to the source or destination. Interestingly, the performance of the (Alt)MuStR1 methods are slightly dominated by 'Pth-High', when relay is positioned very close to the source. The reason is that in such a situation the bottleneck shifts to the relay-destination path as the source-relay channel is very strong and is not degraded by the impact of distortion from the self-interference path. Nevertheless, the distortion awareness

in (Alt)MuStR1 destructively limits the performance of the relay-destination path in order to avoid distortion on the relay receiver. It is worth mentioning that this mismatch does not appear for the GP method, since the final SDNR is considered as the optimization objective which remains relevant for any relay position.

In Fig. 13 the impact of the self-interference channel intensity is depicted. It is observed that the performance of the FD relay operation, for all design methods, degrades as the  $\rho_{rr}$  increase while the performance of the HD method is not changed. As expected, the performance of the methods with perfect hardware assumptions degrades faster compared to the proposed methods. Moreover, the performance of the proposed AltMuStR1 method remains close to that of GP, for different values of the self-interference channel intensity.

## VIII. CONCLUSION

The impact of hardware inaccuracies is of particular importance for an FD transceiver, due to the high strength of the self-interference channel. In particular, for an FD AF relaying system, such impact is significant due to the interdependency of the relay transmit power, as well as the residual self-interference, which results in a distortion loop effect. In this work, we have analytically observed the aforementioned effect, and proposed optimization strategies to alleviate the resulting degradation. It is observed that the proposed GP algorithm can be considered as the performance benchmark, though, imposing a high computational complexity. On the other hand, the proposed (Alt)MuStR1 methods provide a significant reduction in the complexity, at the expense of a slightly lower performance. In particular, the comparison to the available schemes in the literature reveals that for a system with a small thermal noise variance, or a high power or transceiver inaccuracy, the application of a distortion-aware design is essential.

## APPENDIX A

### OPTIMAL $P_s$ AS A FUNCTION OF $\mathbf{W}$

Let  $\mathbf{W}$  and  $\mathbf{z}$  be the fixed (given) relay amplification and receive filter, respectively. From (15)-(20), the SDNR at the destination can be written as a function of  $P_s$

$$\text{SDNR}(P_s) = \frac{\alpha_1 P_s}{\alpha_2 P_s + \alpha_3}, \quad (62)$$

where  $\alpha_1, \alpha_2, \alpha_3 \in \mathbb{R}^+$ , such that

$$\begin{aligned} \alpha_1 &:= \mathbf{z}^H \mathbf{H}_{rd} \mathbf{W} \mathbf{h}_{sr} \mathbf{h}_{sr}^H \mathbf{W}^H \mathbf{H}_{rd}^H \mathbf{z}, \\ \alpha_2 &:= \mathbf{q}(\mathbf{W}, \mathbf{z}) \text{vec}(\mathbf{h}_{sr} \mathbf{h}_{sr}^H) + \mathbf{z}^H \mathbf{h}_{sd} \mathbf{h}_{sd}^H \mathbf{z} - \alpha_1, \\ \alpha_3 &:= \mathbf{z}^H \mathbf{z} \sigma_{nd}^2 + \mathbf{q}(\mathbf{W}, \mathbf{z}) \text{vec}(\sigma_{nr}^2 \mathbf{I}_{M_r}), \\ \mathbf{q}(\mathbf{W}, \mathbf{z}) &:= (\mathbf{z}^T \otimes \mathbf{z}^H) (\mathbf{H}_{rd}^* \otimes \mathbf{H}_{rd}) (\mathbf{I}_{M_t^2} + \kappa \mathbf{S}_D^{M_t}) \\ &\quad \times (\mathbf{I}_{M_t^2} - (\mathbf{W}^* \otimes \mathbf{W}) \mathbf{C})^{-1} (\mathbf{W}^* \otimes \mathbf{W}) (\mathbf{I}_{M_t^2} + \beta \mathbf{S}_D^{M_t}). \end{aligned} \quad (63)$$

It is observed, by taking the first and second order derivatives of the obtained function in (62), that SDNR is an increasing and concave function over  $P_s$ , which concludes the proof.

APPENDIX B  
EQUIVALENT TRANSMIT DISTORTION CHANNEL  
EXPRESSION

Via the application of  $\mathbf{w}_{\text{tx}}$ , the collective received distortion power due to the relay transmission, here denoted as  $\theta_1$ , is written as

$$\begin{aligned}
\theta_1 &= P_{r,\max} \kappa \text{tr} \left( \mathbf{H}_{\text{rr}} \text{diag} (\mathbf{w}_{\text{tx}} \mathbf{w}_{\text{tx}}^H) \mathbf{H}_{\text{rr}}^H + \mathbf{H}_{\text{rd}} \text{diag} (\mathbf{w}_{\text{tx}} \mathbf{w}_{\text{tx}}^H) \mathbf{H}_{\text{rd}}^H \right) \\
&+ P_{r,\max} \beta \text{tr} \left( \text{diag} (\mathbf{H}_{\text{rr}} \mathbf{w}_{\text{tx}} \mathbf{w}_{\text{tx}}^H \mathbf{H}_{\text{rr}}^H) \right) \\
&= \sum_{i \in \mathbb{F}_{M_t}} \sum_{X \in \{\text{rr}, \text{rd}\}} P_{r,\max} \kappa \text{tr} (\mathbf{H}_X \mathbf{\Gamma}_i^{M_t} \mathbf{w}_{\text{tx}} \mathbf{w}_{\text{tx}}^H \mathbf{\Gamma}_i^{M_t} \mathbf{H}_X^H) \\
&+ \sum_{i \in \mathbb{F}_{M_t}} P_{r,\max} \beta \text{tr} (\mathbf{\Gamma}_i^{M_t} \mathbf{H}_{\text{rr}} \mathbf{w}_{\text{tx}} \mathbf{w}_{\text{tx}}^H \mathbf{H}_{\text{rr}}^H \mathbf{\Gamma}_i^{M_t}) \\
&= \kappa P_{r,\max} \sum_{i \in \mathbb{F}_{M_t}} \sum_{X \in \{\text{rr}, \text{rd}\}} \left\| \mathbf{H}_X \mathbf{\Gamma}_i^{M_t} \mathbf{w}_{\text{tx}} \right\|_2^2 \\
&+ \beta P_{r,\max} \sum_{i \in \mathbb{F}_{M_t}} \left\| \mathbf{\Gamma}_i^{M_t} \mathbf{H}_{\text{rr}} \mathbf{w}_{\text{tx}} \right\|_2^2 \\
&= P_{r,\max} \left\| \begin{bmatrix} \lfloor \sqrt{\kappa} \mathbf{H}_X \mathbf{\Gamma}_i^{M_t} \mathbf{w}_{\text{tx}} \rfloor_{i \in \mathbb{F}_{M_t}, X \in \{\text{rr}, \text{rd}\}} \\ \lfloor \sqrt{\beta} \mathbf{\Gamma}_i^{M_t} \mathbf{H}_{\text{rr}} \mathbf{w}_{\text{tx}} \rfloor_{i \in \mathbb{F}_{M_t}} \end{bmatrix} \right\|_2^2 \\
&= P_{r,\max} \left\| \underbrace{\begin{bmatrix} \lfloor \sqrt{\kappa} \mathbf{H}_X \mathbf{\Gamma}_i^{M_t} \rfloor_{i \in \mathbb{F}_{M_t}, X \in \{\text{rr}, \text{rd}\}} \\ \lfloor \sqrt{\beta} \mathbf{\Gamma}_i^{M_t} \mathbf{H}_{\text{rr}} \rfloor_{i \in \mathbb{F}_{M_t}} \end{bmatrix}}_{=: \mathbf{H}_{\text{D,tx}}} \mathbf{w}_{\text{tx}} \right\|_2^2,
\end{aligned} \tag{64}$$

where  $\mathbf{\Gamma}_i^M$  is an  $M \times M$  all-zero matrix, except for the  $i$ -th diagonal element equal to one, and  $\mathbf{H}_{\text{D,tx}}$  is viewed as the equivalent distortion channel.

APPENDIX C  
DERIVATION OF (39)-(40) AND THE COEFFICIENTS  
(41)-(45)

The desired signal power at the destination prior to the application of  $\mathbf{z}$ , here denoted as  $\theta_2$ , can be calculated applying the known matrix equalities [46, e.q. (487), (486), (496)] as

$$\begin{aligned}
\theta_2 &= P_s \text{tr} (\mathbf{H}_{\text{rd}} \mathbf{W} \mathbf{h}_{\text{sr}} \mathbf{h}_{\text{sr}}^H \mathbf{W}^H \mathbf{H}_{\text{rd}}^H) \\
&= \omega P_s \text{tr} \left( \mathbf{H}_{\text{rd}} \mathbf{w}_{\text{tx}} \mathbf{w}_{\text{tx}}^H \mathbf{h}_{\text{sr}} \mathbf{h}_{\text{sr}}^H (\mathbf{w}_{\text{tx}} \mathbf{w}_{\text{tx}}^H)^H \mathbf{H}_{\text{rd}}^H \right) \\
&= \omega P_s \mathbf{d}_{M_t}^T \left( (\mathbf{H}_{\text{rd}}^* (\mathbf{w}_{\text{tx}} \mathbf{w}_{\text{tx}}^H)^*) \otimes (\mathbf{H}_{\text{rd}} \mathbf{w}_{\text{tx}} \mathbf{w}_{\text{tx}}^H) \right) \text{vec} (\mathbf{h}_{\text{sr}} \mathbf{h}_{\text{sr}}^H) \\
&= \omega P_s \mathbf{d}_{M_t}^T (\mathbf{H}_{\text{rd}}^* \otimes \mathbf{H}_{\text{rd}}) \tilde{\mathbf{W}} \text{vec} (\mathbf{h}_{\text{sr}} \mathbf{h}_{\text{sr}}^H) \\
&= \omega a_d,
\end{aligned} \tag{65}$$

where  $a_d$  and  $\mathbf{d}_{M_t}$  are respectively defined in (41) and immediately after (45), and  $\tilde{\mathbf{W}} := (\mathbf{w}_{\text{tx}} \mathbf{w}_{\text{tx}}^H)^* \otimes (\mathbf{w}_{\text{tx}} \mathbf{w}_{\text{tx}}^H)$ . Similarly, following (13)-(16) and the matrix identity [46, e.q. (186)] the noise+interference power at destination, here denoted as  $\theta_3$ , is

calculated as

$$\begin{aligned}
\theta_3 &= N - a_d \omega + \text{tr} (\mathbf{H}_{\text{rd}} \mathbb{E} \{ \mathbf{r}_{\text{out}} \mathbf{r}_{\text{out}}^H \} \mathbf{H}_{\text{rd}}^H) \\
&= N - a_d \omega + \mathbf{d}_{M_d}^T (\mathbf{H}_{\text{rd}}^* \otimes \mathbf{H}_{\text{rd}}) \text{vec} (\mathbb{E} \{ \mathbf{r}_{\text{out}} \mathbf{r}_{\text{out}}^H \}) \\
&= N - a_d \omega + \mathbf{d}_{M_d}^T (\mathbf{H}_{\text{rd}}^* \otimes \mathbf{H}_{\text{rd}}) \left( \mathbf{I}_{M_t^2} + \kappa \mathbf{S}_D^{M_t} \right) \\
&\quad \times \left( \mathbf{I}_{M_t^2} - \omega \tilde{\mathbf{W}} \mathbf{C} \right)^{-1} \omega \tilde{\mathbf{W}} \mathbf{c} \\
&= N - a_d \omega + \mathbf{d}_{M_d}^T (\mathbf{H}_{\text{rd}}^* \otimes \mathbf{H}_{\text{rd}}) \left( \mathbf{I}_{M_t^2} + \kappa \mathbf{S}_D^{M_t} \right) \\
&\quad \times \sum_{k \in \{0 \dots \infty\}} (\omega \tilde{\mathbf{W}} \mathbf{C})^k \omega \tilde{\mathbf{W}} \mathbf{c}
\end{aligned} \tag{66}$$

$$\begin{aligned}
&\approx N - a_d \omega + \sum_{k \in \mathbb{F}_K} \mathbf{d}_{M_d}^T (\mathbf{H}_{\text{rd}}^* \otimes \mathbf{H}_{\text{rd}}) \left( \mathbf{I}_{M_t^2} + \kappa \mathbf{S}_D^{M_t} \right) \\
&\quad \times \left( \tilde{\mathbf{W}} \mathbf{C} \right)^{k-1} \tilde{\mathbf{W}} \mathbf{c} \omega^k
\end{aligned} \tag{67}$$

$$\approx a_0 + \sum_{k \in \mathbb{F}_K} a_k \omega^k, \tag{68}$$

where  $K$  represents the approximation order,  $N := \sigma_{\text{nd}}^2 M_d + P_s \|\mathbf{h}_{\text{sd}}\|_2^2$ , and  $a_k$  is defined in (42) and (44). Note that the identity in (67) holds for any feasible relay transmit strategy, see (21b). This stems from the fact that the effect of the distortion components are attenuated after passing through the loop process, i.e.,  $\omega \tilde{\mathbf{W}} \mathbf{C}$ , in each consecutive symbol duration<sup>8</sup>. Following the same arguments as in (66)-(68) we calculate the relay transmit power as

$$\text{tr} (\mathbb{E} \{ \mathbf{r}_{\text{out}} \mathbf{r}_{\text{out}}^H \}) \tag{70}$$

$$\begin{aligned}
&= \mathbf{d}_{M_t}^T \left( \mathbf{I}_{M_t^2} + \kappa \mathbf{S}_D^{M_t} \right) \left( \mathbf{I}_{M_t^2} - \omega \tilde{\mathbf{W}} \mathbf{C} \right)^{-1} \omega \tilde{\mathbf{W}} \mathbf{c} \\
&= \mathbf{d}_{M_t}^T \left( \mathbf{I}_{M_t^2} + \kappa \mathbf{S}_D^{M_t} \right) \sum_{k \in \{0 \dots \infty\}} (\omega \tilde{\mathbf{W}} \mathbf{C})^k \omega \tilde{\mathbf{W}} \mathbf{c}
\end{aligned} \tag{71}$$

$$\approx \sum_{k \in \mathbb{F}_K} \mathbf{d}_{M_t}^T \left( \mathbf{I}_{M_t^2} + \kappa \mathbf{S}_D^{M_t} \right) \left( \tilde{\mathbf{W}} \mathbf{C} \right)^{k-1} \tilde{\mathbf{W}} \mathbf{c} \omega^k \tag{72}$$

$$\approx b_0 + \sum_{k \in \mathbb{F}_K} b_k \omega^k, \tag{73}$$

where  $b_k$  is defined in (45).

ACKNOWLEDGMENT

The authors would like to thank B.Sc. Tianyu Yang, for his assistance in numerical implementations, Subsection VII-B. We would like to thank him for his efforts and commitment.

REFERENCES

- [1] O. Taghizadeh, T. Yang, A. C. Cirik, and R. Mathar, "Distortion-loop-aware amplify-and-forward full-duplex relaying with multiple antennas," in *International Symposium on Wireless Communication Systems (ISWCS'2016)*, Poznan, Poland, Sep. 2016, pp. 54–58.

<sup>8</sup>Otherwise, the impact of distortion is accumulated in time, leading to an infinite distortion power and instability.

- [2] S. Hong, J. Brand, J. Choi, M. Jain, J. Mehlman, S. Katti, and P. Levis, "Applications of self-interference cancellation in 5G and beyond," *IEEE Communications Magazine*, February 2014.
- [3] B. P. Day, A. R. Margetts, D. W. Bliss, and P. Schniter, "Full-duplex bidirectional MIMO: Achievable rates under limited dynamic range," *IEEE Transactions on Signal Processing*, vol. 60, no. 7, pp. 3702–3713, July 2012.
- [4] D. Bharadia and S. Katti, "Full duplex MIMO radios," in *Proceedings of the 11th USENIX Conference on Networked Systems Design and Implementation*, ser. NSDI'14, Berkeley, CA, USA, 2014, pp. 359–372.
- [5] Y. Hua, P. Liang, Y. Ma, A. Cirik, and G. Qian, "A method for broadband full-duplex MIMO radio," *IEEE Signal Processing Letters*, vol. 19, Dec. 2011.
- [6] D. Bharadia, E. McMillin, and S. Katti, "Full duplex radios," in *Proceedings of the ACM SIGCOMM*, Aug. 2013.
- [7] A. K. Khandani, "Two-way (true full-duplex) wireless," in *13th Canadian Workshop on Information Theory (CWIT, 2013)*.
- [8] A. Sabharwal, P. Schniter, D. Guo, D. Bliss, S. Rangarajan, and R. Wichman, "In-band full-duplex wireless: Challenges and opportunities," *Selected Areas in Communications, IEEE Journal on*, vol. 32, no. 9, pp. 1637–1652, Sept 2014.
- [9] T. Riihonen, S. Werner, and R. Wichman, "Mitigation of loopback self-interference in full-duplex MIMO relays," *IEEE Transactions on Signal Processing*, vol. 59, 2011.
- [10] B. Day, A. Margetts, D. Bliss, and P. Schniter, "Full-duplex MIMO relaying: Achievable rates under limited dynamic range," *IEEE Journal on Selected Areas in Communications*, Sep. 2012.
- [11] X. Xia, D. Zhang, K. Xu, W. Ma, and Y. Xu, "Hardware impairments aware transceiver for full-duplex massive MIMO relaying," *Signal Processing, IEEE Transactions on*, vol. 63, no. 24, pp. 6565–6580, Dec 2015.
- [12] E. Antonio-Rodriguez, R. Lopez-Valcarce, T. Riihonen, S. Werner, and R. Wichman, "SINR optimization in wideband full-duplex MIMO relays under limited dynamic range," in *Sensor Array and Multichannel Signal Processing Workshop (SAM), 2014 IEEE 8th*, June 2014.
- [13] B. Zhong, D. Zhang, Z. Zhang, Z. Pan, K. Long, and A. Vasilakos, "Opportunistic full-duplex relay selection for decode-and-forward cooperative networks over rayleigh fading channels," in *IEEE International Conference on Communications (ICC)*, June 2014.
- [14] E. Antonio-Rodriguez, R. Lopez-Valcarce, T. Riihonen, S. Werner, and R. Wichman, "Subspace-constrained SINR optimization in MIMO full-duplex relays under limited dynamic range," in *Signal Processing Advances in Wireless Communications (SPAWC), 2015 IEEE 16th International Workshop on*, June 2015, pp. 281–285.
- [15] O. Taghizadeh and R. Mathar, "Cooperative strategies for distributed full-duplex relay networks with limited dynamic range," in *International Conference on Wireless for Space and Extreme Environments (WiSEE), 2014 IEEE*, Noordwijk, Netherlands, 2014.
- [16] O. Taghizadeh, M. Rothe, A. C. Cirik, and R. Mathar, "Distortion-Loop analysis for Full-Duplex Amplify-and-Forward relaying in cooperative multicast scenarios," in *2015 9th International Conference on Signal Processing and Communication Systems (ICSPCS)*, Cairns, Australia, Dec. 2015, pp. 107–115.
- [17] T. Riihonen, S. Werner, and R. Wichman, "Optimized gain control for single-frequency relaying with loop interference," *IEEE Transactions on Wireless Communications*, 2009.
- [18] L. Jimenez Rodriguez, N. Tran, and T. Le-Ngoc, "Optimal power allocation and capacity of full-duplex AF relaying under residual self-interference," *IEEE Wireless Communications Letters*, April 2014.
- [19] C. Dang, L. Jimenez Rodriguez, N. Tran, S. Shelly, and S. Sastry, "Secrecy capacity of the full-duplex AF relay wire-tap channel under residual self-interference," in *IEEE Wireless Communications and Networking Conference (WCNC)*, March 2015.
- [20] X. Cheng, B. Yu, X. Cheng, and L. Yang, "Two-way full-duplex amplify-and-forward relaying," in *IEEE Military Communications Conference, MILCOM*, Nov 2013.
- [21] M. Duarte, C. Dick, and A. Sabharwal, "Experiment-driven characterization of full-duplex wireless systems," *IEEE Transactions on Wireless Communications*, December 2012.
- [22] K. Lee, H. Kwon, M. Jo, H. Park, and Y. Lee, "MMSE-based optimal design of full-duplex relay system," in *IEEE Vehicular Technology Conference (VTC Fall)*, Sept 2012.
- [23] O. Somekh, O. Simeone, H. V. Poor, and S. Shamai, "Cellular systems with full-duplex amplify-and-forward relaying and cooperative base-stations," in *2007 IEEE International Symposium on Information Theory*, June 2007, pp. 16–20.
- [24] Z. Wen, X. Liu, N. C. Beaulieu, R. Wang, and S. Wang, "Joint source and relay beamforming design for full-duplex MIMO AF relay SWIPT systems," *IEEE Communications Letters*, vol. 20, no. 2, pp. 320–323, Feb 2016.
- [25] H. Suraweera, I. Krikidis, G. Zheng, C. Yuen, and P. Smith, "Low-complexity end-to-end performance optimization in MIMO full-duplex relay systems," *IEEE Transactions on Wireless Communications*, vol. 13, no. 2, pp. 913–927, Feb. 2014.
- [26] D. Choi and D. Park, "Effective self interference cancellation in full duplex relay systems," *Electronics Letters*, vol. 48, no. 2, pp. 129–130, Jan. 2012.
- [27] B. Chun and H. Park, "A spatial-domain joint-nulling method of self-interference in full-duplex relays," *Communications Letters, IEEE*, vol. 16, no. 4, pp. 436–438, April 2012.
- [28] C. Shang, P. Smith, G. Woodward, and H. Suraweera, "Linear transceivers for full duplex MIMO relays," in *Communications Theory Workshop (AusCTW), 2014 Australian*, Feb 2014, pp. 11–16.
- [29] U. Ugurlu, T. Riihonen, and R. Wichman, "Optimized in-band full-duplex MIMO relay under single-stream transmission," *Vehicular Technology, IEEE Transactions on*, no. 99, pp. 1–1, Jan. 2015.
- [30] Q. Shi, M. Hong, X. Gao, E. Song, Y. Cai, and W. Xu, "Joint source-relay design for full-duplex MIMO AF relay systems," *IEEE Transactions on Signal Processing*, vol. 64, no. 23, pp. 6118–6131, Dec 2016.
- [31] O. Taghizadeh, J. Zhang, and M. Haardt, "Transmit beamforming aided amplify-and-forward MIMO full-duplex relaying with limited dynamic range," *Signal Processing*, 2016.
- [32] Y. Y. Kang, B.-J. Kwak, and J. H. Cho, "An optimal full-duplex AF relay for joint analog and digital domain self-interference cancellation," *Communications, IEEE Transactions on*, vol. 62, no. 8, pp. 2758–2772, Aug 2014.
- [33] H. Shen, W. Xu, and C. Zhao, "Transceiver optimization for full-duplex massive MIMO AF relaying with direct link," *IEEE Access*, vol. 4, pp. 8857–8864, 2016.
- [34] T. Guo and B. Wang, "Joint transceiver beamforming design for end-to-end optimization in full-duplex MIMO relay system with self-interference," *IEEE Communications Letters*, vol. 20, no. 9, pp. 1733–1736, Sept 2016.
- [35] G. Santella and F. Mazzenga, "A hybrid analytical-simulation procedure for performance evaluation in M-QAM-OFDM schemes in presence of nonlinear distortions," *IEEE Trans. Veh. Technol.*, vol. 47, pp. 142–151, 1998.
- [36] H. Suzuki, T. V. A. Tran, I. B. Collings, G. Daniels, and M. Hedley, "Transmitter noise effect on the performance of a MIMO-OFDM hardware implementation achieving improved coverage," *IEEE J. Sel. Areas in Communication*, vol. 26, pp. 867–876, Aug. 2008.
- [37] W. Namgoong, "Modeling and analysis of nonlinearities and mismatches in AC-coupled direct-conversion receiver," *IEEE Trans. Wireless Commun.*, vol. 47, pp. 163–173, Jan. 2005.
- [38] U. Siddique, H. Tabassum, E. Hossain, and D. I. Kim, "Wireless backhauling of 5G small cells: challenges and solution approaches," *IEEE Wireless Communications*, vol. 22, no. 5, pp. 22–31, October 2015.

- [39] D. P. M. Osorio, E. E. B. Olivo, H. Alves, J. C. S. S. Filho, and M. Latva-aho, "Exploiting the direct link in full-duplex amplify-and-forward relaying networks," *IEEE Signal Processing Letters*, vol. 22, no. 10, pp. 1766–1770, Oct 2015.
- [40] G. E. Bottomley, T. Ottosson, and Y. P. E. Wang, "A generalized RAKE receiver for interference suppression," *IEEE Journal on Selected Areas in Communications*, vol. 18, no. 8, pp. 1536–1545, Aug 2000.
- [41] T. Riihonen, S. Werner, and R. Wichman, "Hybrid full-duplex/half-duplex relaying with transmit power adaptation," *IEEE Transactions on Wireless Communications*, vol. 10, no. 9, pp. 3074–3085, September 2011.
- [42] D. P. Bertsekas, *Nonlinear programming*. Athena scientific Belmont, 1999.
- [43] A. Cohen, "Stepsize analysis for descent methods," in *Proceedings of IEEE 12th International Symposium on Adaptive Processes*, Dec. 1973.
- [44] R.-C. Li, "Rayleigh quotient based optimization methods for eigenvalue problems," *Matrix Functions and Matrix Equations*, vol. 19, pp. 76–108, 2014.
- [45] Y. Huang and D. P. Palomar, "Rank-constrained separable semidefinite programming with applications to optimal beamforming," *IEEE Transactions on Signal Processing*, vol. 58, pp. 664–678, Feb. 2010.
- [46] S. Petersen and M. Pedersen, *Matrix Cookbook*, 2008.